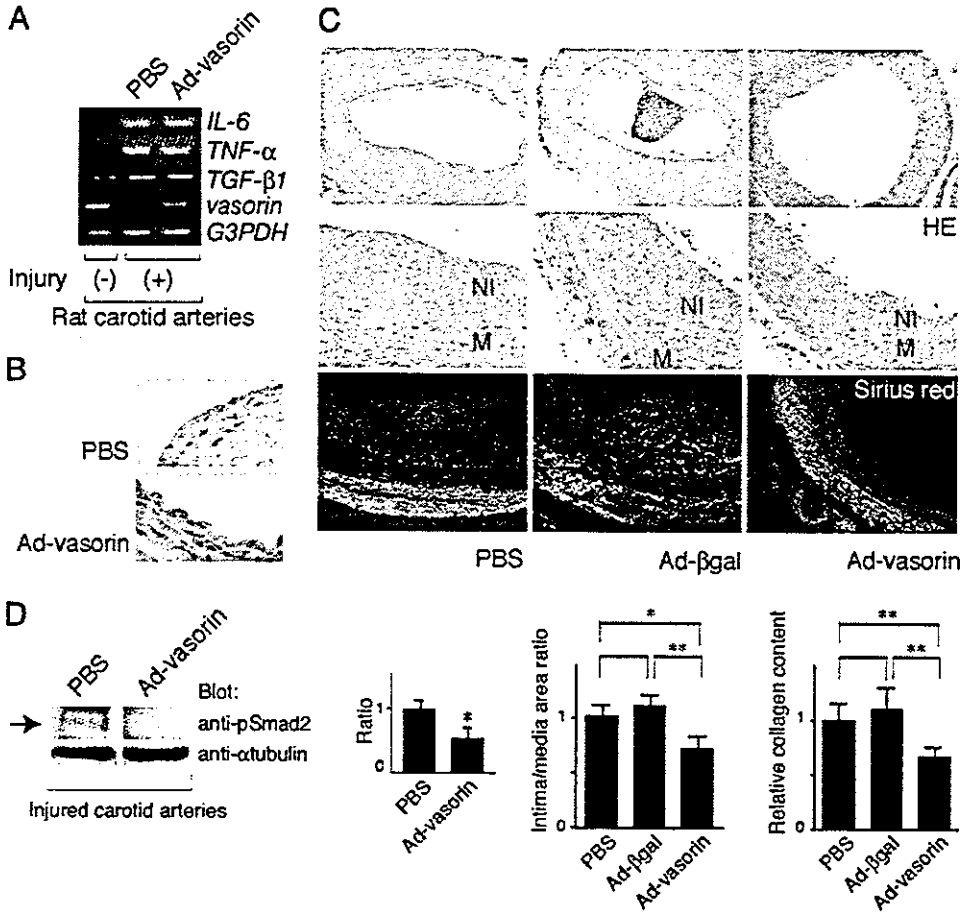

Fig. 5. Vasorin expression was down-regulated during vessel repair after arterial injury, and reversal of vasorin down-regulation significantly reduced neointimal formation, at least in part, by attenuating TGF-β signaling *in vivo*. (*A*) Rat carotid arteries were harvested at 3 days after injury to examine the expression levels of *vasorin* by semiquantitative RT-PCR analysis. Down-regulation of *vasorin* expression was induced by mechanical vascular injury, and Ad-vasorin treatment partially reversed this down-regulation. In contrast to vasorin, the expression of TGF-β1, TNF-α, and IL-6 was up-regulated by vascular injury and was not altered by vasorin administration. GAPDH was used as an internal control. (*B*) Vessels treated with Ad-vasorin were harvested 3 days afterward and were subjected to immunostaining to confirm protein expression by using the anti-Flag antibody. (*C*) Effects of Ad-vasorin on neointimal formation in rat carotid arteries at 14 days after injury ($n = 5$ arteries for each group). Representative hematoxylin/eosin-stained cross sections (*Top* and *Middle*) and Sirius red-stained cross sections (*Bottom*) of balloon-injured arteries treated with PBS (*Left*), Ad-β-galactosidase (*Center*), and Ad-vasorin (*Right*) are shown. (*Middle*) Partial magnifications of the respective *Top* images. Ad-vasorin administration significantly reduced the intima/media area ratio of injured arteries and collagen content in the lesions ($P < 0.01$), as compared with Ad-β-galactosidase administration. NI, neointima; M, media; HE, hematoxylin/eosin. *, $P < 0.05$; **, $P < 0.01$. (*D*) The inhibitory effects of vasorin administration on TGF-β signaling *in vivo*. Arteries were harvested 3 days after injury and were subjected to Western blot analysis by using the anti-phospho-Smad2 antibody. Representative data are shown. Smad2 phosphorylation was significantly reduced in all Ad-vasorin-treated arteries ($P < 0.05$). The blots were stripped and reprobed with the anti-α-tubulin antibody to ensure equal loading of proteins. The relative intensities of phospho-Smad2 bands were measured by densitometric scanning from three independent experiments. *, $P < 0.05$.

ward to examine the expression of vasorin by RT-PCR analysis (Fig. 5*A*), immunostaining (Fig. 5*B*), and Western blot analysis (data not shown). Ad-mediated *vasorin* gene transfer was successful (Fig. 5 *A* and *B*), and the expression of TGF-β, TNF-α, and IL-6 was not altered by vasorin administration (Fig. 5*A*). Second, arteries were harvested to assess the effect of *vasorin* gene transfer on neointimal formation ($n = 5$ arteries for each group) at 14 days after injury. The administration of Ad-vasorin significantly reduced the intima/media area ratio of injured arteries by 35% ($P < 0.01$), as compared with the administration of Ad-β-galactosidase (Fig. 5*C*), suggesting that restoration of vasorin expression had a significant inhibitory effect on neointimal formation. Because TGF-β stimulates extracellular matrix protein synthesis, and also functions as an antiinflammatory cytokine, we examined collagen content and leukocyte infiltration in the lesions quantitatively, by using Sirius red staining and CD45 staining, respectively. As shown in Fig. 5*C Lower*, vasorin administration significantly reduced collagen content in the lesions ($P < 0.01$), whereas leukocyte infiltration was not altered (data not shown).

Finally, we investigated whether *in vivo* vasorin administration inhibits TGF-β signaling in the vessel wall. Balloon-injured rat carotid arteries treated with Ad-vasorin were subjected to Western blot analysis, by using the anti-phospho-Smad2 antibody, when the fibroproliferative activity of VSMCs peaked (3 days after injury). Smad2 phosphorylation was significantly reduced in Ad-vasorin-treated arteries ($P < 0.05$; Fig. 5*D*). These results suggest that enhanced TGF-β signaling after vascular injury (Fig. 5*A*) is significantly inhibited by *in vivo* vasorin administration, and that vasorin inhibits neointimal formation at least in part by modulating TGF-β signaling in the vessel wall.

Discussion

VSMCs respond to various growth factors, and the best investigated situation in which VSMCs proliferate and produce extracellular matrix proteins *in vivo* is after vascular injury.

Whereas the rat carotid arterial balloon-injury model has been studied extensively, the underlying mechanisms that regulate vessel repair and neointimal formation appear to be the same in other arteries and in other species, including humans. The phenotype of VSMCs following arterial injury is similar to that observed during embryonic angiogenesis, and molecular mechanisms that regulate VSMC differentiation during embryonic development are thought to be recapitulated during vessel repair. *Vasorin* gene expression was developmentally regulated (Fig. 3 *A–D*), and, consistent with this finding, *vasorin* was down-regulated during vessel repair after arterial injury (Fig. 5*A*). This finding suggests its involvement in injury-induced vascular lesion formation. Therefore, we explored the *in vivo* functions of vasorin, by using a rat arterial balloon-injury model combined with Ad-mediated *in vivo* gene transfer. As shown in Fig. 5*C*, reversal of vasorin down-regulation had a significant inhibitory effect on neointimal formation. These results indicate that down-regulation of vasorin expression contributes to the fibroproliferative response to vascular injury.

Numerous factors that regulate VSMC activity have been studied in the arterial-injury model, and the results of these investigations suggest the importance of pathological extracellular stimuli, such as the renin-angiotensin system, catecholamines, EGF, platelet-derived growth factor (PDGF), insulin-like growth factor I, endothelin 1, TGF-β, and oxidative stress. TGF-β is a context-dependent pleiotropic cytokine, which plays a key role in the vascular response to injury. Several studies using gene transfer techniques have shown that locally enhanced TGF-β signaling enables matrix-rich neointima to develop in uninjured normal arteries of rats (11, 12). In contrast, localized blockade of TGF-β signaling results in the inhibition of neointimal formation, accompanied by reduced extracellular matrix synthesis in a rat balloon-injury model (13, 14). Of clinical relevance is the observation that the expression levels of TGF-β mRNA in restenotic lesions are higher than those in primary atherosclerotic lesions (15). These investigations indicate that TGF-β functions as a fibrogenic cytokine in a balloon-injury model, and apparently aggravates neointimal formation by promoting fibrosis. In this paper, we found that vasorin directly binds to TGF-β and negatively modulates TGF-β signaling in the vessel wall (Figs. 4 and 5*D*). Considering the functional role of TGF-β in this model, it is reasonably assumed that the *in vivo* phenotype induced by Ad-vasorin administration is mediated at least in part by the inhibitory effects of vasorin on TGF-β signaling in the vessel wall.

The extracellular region of vasorin is composed of ten tandem arrays of an LRR, an EGF-like domain, and a fibronectin type III-like domain, that are known to be involved in protein–protein interactions (Fig. 1*B*). Secreted and cell-surface molecules containing those domains, such as extracellular matrix proteins and adhesion molecules, sometimes have multiple binding partners. PDGF and TGF-β are prominent growth factors that have been suggested to play an important role in neointimal formation after arterial injury, and we demonstrated here that vasorin directly binds to TGF-β, but not to PDGF (Fig. 4*B*). However, it is possible that vasorin has other binding partners and that vasorin affects not only TGF-β signaling but also other signaling pathways, through another yet-to-be-identified mechanism. Further investigations will be needed to clarify these issues.

In the present study, we found that down-regulation of vasorin expression was induced by acute vascular injury, and that reversal of vasorin down-regulation during vessel repair inhibits neointimal formation, at least in part, by modulating cellular responses to TGF-β. These data raise a possibility that the gene expression profile of cell-surface molecules is changed by mechanical vascular injury, and that altered cellular responses to growth factors in dedifferentiated VSMCs are in part due to this change. Thus, identification and modification of the pivotal gene expression of cell-surface molecules in VSMCs may be a potential therapeutic approach to vascular fibroproliferative disorders.

We thank Dr. G. K. Owens for A404 cells, M. Ohara for language assistance, and Drs. H. Ono and H. Ogasawara for valuable advice. This work was also supported in part by grants from the Ministry of Education, Science, Technology, Sports, and Culture of Japan. The Division of Hematopoietic Factors was supported in part by the Chugai Pharmaceutical Company, Ltd.

1. Tashiro, K., Tada, H., Heilker, R., Shirozu, M., Nakano, T. & Honjo, T. (1993) *Science* **261**, 600–603.
2. Klein, R. D., Gu, Q., Goddard, A. & Rosenthal, A. (1996) *Proc. Natl. Acad. Sci. USA* **93**, 7108–7113.
3. Kojima, T. & Kitamura, T. (1999) *Nat. Biotechnol.* **17**, 487–490.
4. Nosaka, T., Kawashima, T., Misawa, K., Ikuta, K., Mui, A. L. & Kitamura, T. (1999) *EMBO J.* **18**, 4754–4765.
5. Chamley-Campbell, J., Campbell, G. R. & Ross, R. (1979) *Physiol. Rev.* **59**, 1–61.
6. Clowes, A. W., Reidy, M. A. & Clowes, M. M. (1983) *Lab. Invest.* **49**, 327–333.
7. Manabe, I. & Owens, G. (2001) *Circ. Res.* **88**, 1127–1134.
8. Kajava, A. V. (1998) *J. Mol. Biol.* **277**, 519–527.
9. Iozzo, R. V. (1999) *J. Biol. Chem.* **274**, 18843–18846.
10. Yamaguchi, Y., Mann, D. M. & Ruoslahti, E. (1990) *Nature* **346**, 281–284.
11. Nabel, E. G., Shum, L., Pompili, V. J., Yang, Z. Y., San, H., Shu, H. B., Liptay, S., Gold, L., Gordon, D., Derynck, R., *et al.* (1993) *Proc. Natl. Acad. Sci. USA* **90**, 10759–10763.
12. Schulick, A. H., Taylor, A. J., Zuo, W., Qiu, C. B., Dong, G., Woodward, R. N., Agah, R., Roberts, A. B., Virmani, R. & Dichek, D. A. (1998) *Proc. Natl. Acad. Sci. USA* **95**, 6983–6988.
13. Yamamoto, K., Morishita, R., Tomita, N., Shimozato, T., Nakagami, H., Kikuchi, A., Aoki, M., Higaki, J., Kaneda, Y. & Ogihara, T. (2000) *Circulation* **102**, 1308–1314.
14. Kingston, P. A., Sinha, S., David, A., Castro, M. G., Lowenstein, P. R. & Heagerty, A. M. (2001) *Circulation* **104**, 2595–2601.
15. Nikol, S., Isner, J. M., Pickering, J. G., Kearney, M., Leclerc, G. & Weir, L. (1992) *J. Clin. Invest.* **90**, 1582–1592.

nature medicine

G-CSF prevents cardiac remodeling after myocardial infarction by activating the Jak-Stat pathway in cardiomyocytes

Mutsuo Harada[1,4], Yingjie Qin[1,4], Hiroyuki Takano[1,4], Tohru Minamino[1,4], Yunzeng Zou[1], Haruhiro Toko[1], Masashi Ohtsuka[1], Katsuhisa Matsuura[1], Masanori Sano[1], Jun-ichiro Nishi[1], Koji Iwanaga[1], Hiroshi Akazawa[1], Takeshige Kunieda[1], Weidong Zhu[1], Hiroshi Hasegawa[1], Keita Kunisada[2], Toshio Nagai[1], Haruaki Nakaya[3], Keiko Yamauchi-Takihara[2] & Issei Komuro[1]

Granulocyte colony-stimulating factor (G-CSF) was reported to induce myocardial regeneration by promoting mobilization of bone marrow stem cells to the injured heart after myocardial infarction, but the precise mechanisms of the beneficial effects of G-CSF are not fully understood. Here we show that G-CSF acts directly on cardiomyocytes and promotes their survival after myocardial infarction. G-CSF receptor was expressed on cardiomyocytes and G-CSF activated the Jak/Stat pathway in cardiomyocytes. The G-CSF treatment did not affect initial infarct size at 3 d but improved cardiac function as early as 1 week after myocardial infarction. Moreover, the beneficial effects of G-CSF on cardiac function were reduced by delayed start of the treatment. G-CSF induced antiapoptotic proteins and inhibited apoptotic death of cardiomyocytes in the infarcted hearts. G-CSF also reduced apoptosis of endothelial cells and increased vascularization in the infarcted hearts, further protecting against ischemic injury. All these effects of G-CSF on infarcted hearts were abolished by overexpression of a dominant-negative mutant Stat3 protein in cardiomyocytes. These results suggest that G-CSF promotes survival of cardiac myocytes and prevents left ventricular remodeling after myocardial infarction through the functional communication between cardiomyocytes and noncardiomyocytes.

Myocardial infarction is the most common cause of cardiac morbidity and mortality in many countries, and left ventricular remodeling after myocardial infarction is important because it causes progression to heart failure. Several cytokines including G-CSF, erythropoietin and leukemia inhibitory factor have beneficial effects on cardiac remodeling after myocardial infarction[1–5]. In particular, G-CSF markedly improves cardiac function and reduce mortality after myocardial infarction in mice, possibly by regeneration of myocardium and angiogenesis[1,2,6–8]. G-CSF is known to have various functions such as induction of proliferation, survival and differentiation of hematopoietic cells, as well as mobilization of bone marrow cells[9–11]. Although it was reported that bone marrow cells could differentiate into cardiomyocytes and vascular cells, thereby contributing to regeneration of myocardium and angiogenesis in ischemic hearts[12–15], accumulating evidence has questioned these previous reports[16–18]. In this study, we examined the molecular mechanisms of how G-CSF prevents left ventricular remodeling after myocardial infarction.

RESULTS

G-CSF directly acts on cultured cardiomyocytes

G-CSF receptor (G-CSFR, encoded by *CSF3R*) has been reported to be expressed only on blood cells such as myeloid leukemic cells, leukemic cell lines, mature neutrophils, platelets, monocytes and some lymphoid cell lines[9]. To test whether G-CSFR is expressed on mouse cardiomyocytes, we performed a reverse transcription–polymerase chain reaction (RT-PCR) experiment by using specific primers for mouse *Csf3r*. We detected expression of the *Csf3r* gene in the adult mouse heart and cultured neonatal cardiomyocytes (**Fig. 1a**). We next examined expression of G-CSFR protein in cultured cardiomyocytes of neonatal rats by immunocytochemistry. Similar to the previously reported expression pattern of G-CSFR in living cells[19], the immunoreactivity for G-CSFR was localized to the cytoplasm and cell membrane under steady-state conditions in cardiomyocytes (**Fig. 1b**). This immunoreactivity disappeared when the antibody specific for G-CSFR was omitted, validating its specificity (**Fig. 1b**). In addition to cardiomyocytes, we also detected expression of G-CSFR on cardiac fibroblasts by immunocytochemistry (see **Supplementary Fig. 1** online) and RT-PCR (**Supplementary Fig. 2** online).

The binding of G-CSF to its receptor has been reported to evoke signal transduction by activating the receptor-associated Janus family tyrosine kinases (JAK) and signal transducer and activator of transcription (STAT) proteins in hematopoietic cells[9,10]. In particular, STAT3

[1]Department of Cardiovascular Science and Medicine, Chiba University Graduate School of Medicine, 1-8-1 Inohana, Chuo-ku, Chiba 260-8670, Japan. [2]Department of Molecular Medicine, Osaka University Medical School, Osaka University, 2-2 Yamadaoka, Suita, Osaka 565-0871, Japan. [3]Department of Pharmacology, Chiba University Graduate School of Medicine, 1-8-1 Inohana, Chuo-ku, Chiba 260-8670, Japan. [4]These authors contributed equally to this work. Correspondence should be addressed to I.K. (komuro-tky@umin.ac.jp).

Published online 20 February 2005; doi:10.1038/nm1199

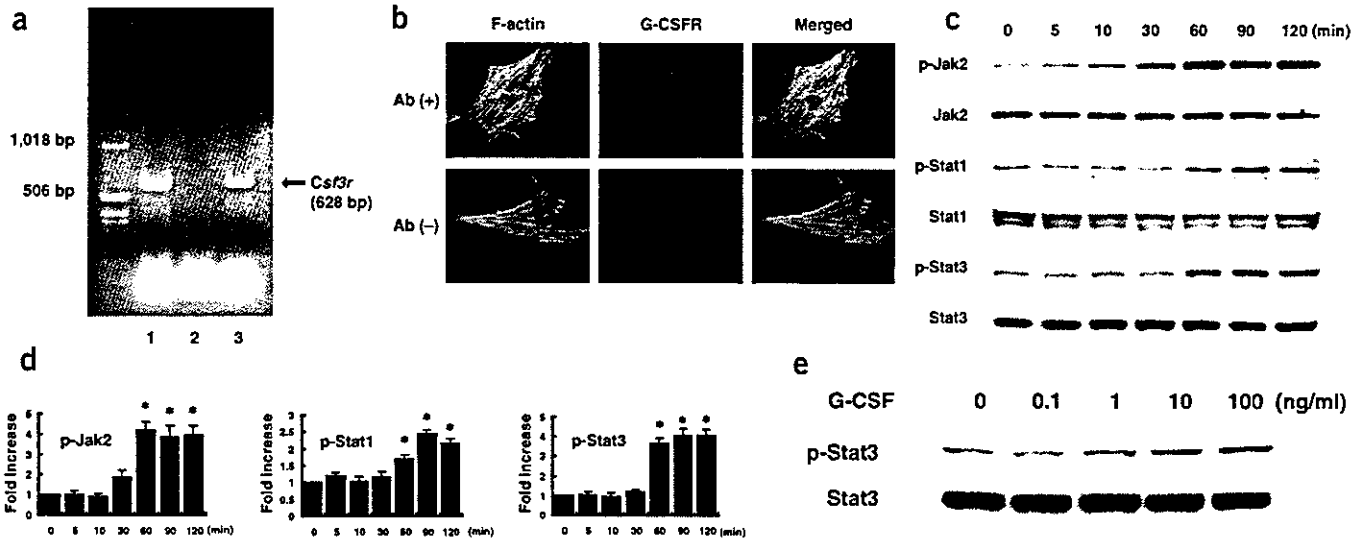

Figure 1 Expression of G-CSFR and the G-CSF-evoked signal transduction in cultured cardiomyocytes. (a) RT-PCR for mouse *Csf3r*. Expression of *Csf3r* was detected in the adult mouse heart (lane 1) and cultured cardiomyocytes of neonatal mice (lane 3). In lane 2, reverse transcription products were omitted to exclude the possibility of false-positive results from contamination. (b) Immunocytochemical staining for G-CSFR. Cardiomyocytes from neonatal rats were incubated with antibody to G-CSFR (red) and phalloidin (green) (upper panel). In the absence of antibody to G-CSFR, no signal was detected (lower panel). Original magnification, ×1,000. (c) G-CSF induces phosphorylation of Jak2, Stat1 and Stat3 in a time-dependent manner in cultured cardiomyocytes. (d) Quantification of Jak2, Stat1 and Stat3 activation by G-CSF stimulation as compared with control (time = 0). $^*P < 0.05$ versus control ($n = 3$). (e) G-CSF induces phosphorylation and activation of Stat3 in a dose-dependent manner in cultured cardiomyocytes.

has been reported to contribute to G-CSF-induced myeloid differentiation and survival[20,21]. We therefore examined whether G-CSF activates the Jak-Stat signaling pathway in cultured cardiomyocytes. G-CSF (100 ng/ml) significantly induced phosphorylation and activation of Jak2 and Stat3, and to a lesser extent, Stat1 but not Jak1, Tyk2 or Stat5 in a dose-dependent manner (**Fig. 1c–e** and data not shown), suggesting that G-CSFR on cardiomyocytes is functional.

We next examined whether G-CSF confers direct protective effects on cardiomyocytes as it prevents hematopoietic cells from apoptotic death[21]. We exposed cardiomyocytes to 0.1 mM H_2O_2 in the absence or presence of G-CSF and examined cardiomyocyte apoptosis by staining with annexin V[22,23]. Pretreatment with G-CSF significantly reduced the number of H_2O_2-induced annexin V–positive cells compared with cells that were not given the G-CSF pretreatment

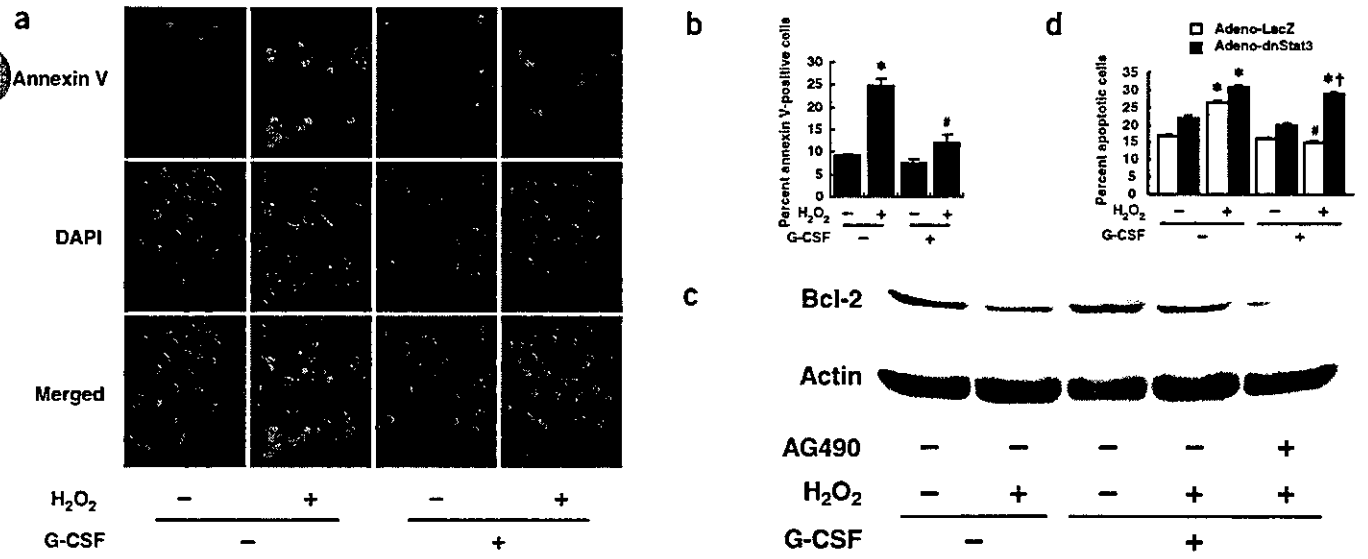

Figure 2 Suppression of H_2O_2-induced cardiomyocyte apoptosis by G-CSF. (a) Detection of apoptosis by Cy3-labeled annexin V. Red fluorescence shows apoptotic cardiomyocytes stained with Cy3-labeled annexin V. Nuclei were counterstained with DAPI staining (blue). Original magnification, ×400. (b) Quantitative analysis of apoptotic cells. The vertical axis indicates the ratio of the annexin V–positive cell number relative to that of DAPI-positive nuclei. $^*P < 0.01$ versus nontreated cells, $^\#P < 0.05$ versus H_2O_2-treated cells without G-CSF ($n = 3$). (c) G-CSF prevents H_2O_2-induced downregulation of Bcl-2 expression ($n = 3$). (d) Inhibition of antiapoptotic effects of G-CSF by Adeno-dnStat3. Bar graphs represent quantitative analysis of the apoptotic cell number relative to the total cell number. $^*P < 0.001$ versus H_2O_2 (–)/G-CSF (–), $^\#P < 0.001$ versus H_2O_2 (+)/G-CSF (–), $^\dagger P < 0.001$ versus H_2O_2 (+)/G-CSF (+)/Adeno-LacZ ($n = 3$).

(Fig. 2a,b). To investigate the molecular mechanism of how G-CSF exerts an antiapoptotic effect on cultured cardiomyocytes, we examined expression of the Bcl-2 protein family, known target molecules of the Jak-Stat pathway[24], by western blot analysis. Expression levels of antiapoptotic proteins such as Bcl-2 and Bcl-xL were lower when cardiomyocytes were subjected to H_2O_2 (Fig. 2c and data not shown), and this reduction was considerably inhibited by G-CSF pretreatment (Fig. 2c). AG490, an inhibitor of Jak2, abolished G-CSF-induced Bcl-2 expression (Fig. 2c) but did not affect its basal levels (**Supplementary** Fig. 3 online), suggesting a crucial role of the Jak-Stat pathway in inducing survival of cardiomyocytes by G-CSF. To further elucidate the involvement of the Jak-Stat pathway in the protective effects of G-CSF on cardiomyocytes, we transduced cultured cardiomyocytes with adenovirus encoding dominant-negative Stat3 (Adeno-dnStat3). G-CSF treatment significantly reduced apoptosis induced by H_2O_2 in Adeno-LacZ-infected cardiomyocytes (Fig. 2d). This effect was abolished by introduction of Adeno-dnStat3 (Fig. 2d), suggesting that Stat3 mediates the protective effects of G-CSF on H_2O_2-induced cardiomyocyte apoptosis.

Effects of G-CSF on cardiac function after myocardial infarction

Consistent with the *in vitro* data, G-CSF enhanced activation of Stat3 in the infarcted heart (Fig. 3a). Notably, the levels of G-CSFR were markedly increased after myocardial infarction in cardiomyocytes (**Supplementary Fig. 4** online), which may enhance the effects of G-CSF on the infarcted heart. To elucidate the role of G-CSF-induced Stat3 activation in cardiac remodeling, we produced myocardial infarction in transgenic mice which express dominant-negative Stat3 in cardiomyocytes under the control of the α-myosin heavy chain promoter (dnStat3-Tg). Administration of G-CSF was started at the time of coronary artery ligation (day 0) until day 4 in transgenic mice; we termed this group Tg-G mice. A control group of dnStat3-Tg mice given myocardial infarction received saline (Tg-cont) instead of G-CSF. We also included two groups of wild-type mice given myocardial infarction treated with G-CSF (Wt-G) or saline (Wt-cont). At 2 weeks after myocardial infarction, we assessed the morphology by histological analysis and measured cardiac function by echocardiography and catheterization analysis. The infarct area was significantly smaller in the Wt-G group than the Wt-cont group (Fig. 3b). The Wt-G group also showed less left ventricular end-diastolic dimension (LVEDD) and better fractional shortening as assessed by echocardiography, and lower end-diastolic pressure (LVEDP) and better $+dp/dt$ and $-dp/dt$ as assessed by cardiac catheterization compared with Wt-cont (Fig. 3c). The beneficial effects of G-CSF on cardiac function were dose dependent and were significantly reduced by delayed start of the treatment (Fig. 3d,e and **Supplementary Fig. 5** online). Moreover, its favorable effects on cardiac function became evident within 1 week after the treatment (Fig. 3f). Disruption of the Stat3 signaling pathway in cardiomyocytes abolished the protective effects of G-CSF. There was no significant difference in LVEDD, fractional shortening, LVEDP, $+dp/dt$ and $-dp/dt$ between Tg-G and Tg-cont (Fig. 3c). We obtained similar results from infarcted female hearts (Fig. 3g). These results suggest that G-CSF protects the heart after myocardial infarction at least in part by directly activating Stat3 in cardiomyocytes, which is a gender-independent effect. We have previously shown that treatment with G-CSF significantly ($P < 0.05$) decreased myocardial infarction–related mortality of wild-type mice[2]. In contrast, there were no significant differences in mortality between G-CSF-treated and saline-treated dnStat3-Tg mice (data not shown).

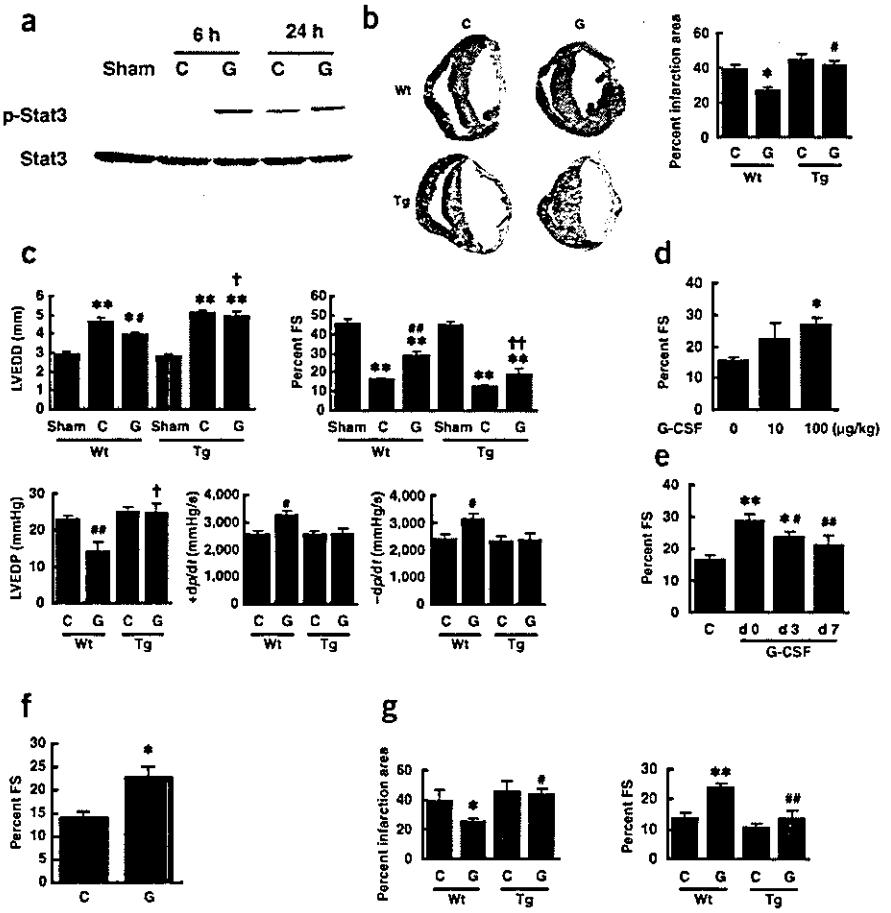

Figure 3 Effects of G-CSF on cardiac function after myocardial infarction. (a) Stat3 activation in the infarcted hearts. We operated on wild-type mice to induce myocardial infarction and treated them with G-CSF (G) or saline (C). (b) Masson trichrome staining of wild-type (Wt) and dnStat3-Tg (Tg) hearts. $^*P < 0.001$ versus Wt-cont, $^\#P < 0.001$ versus Wt-G ($n = 11$–15). (c) G-CSF treatment preserves cardiac function after myocardial infarction. $^*P < 0.01$, $^{**}P < 0.001$ versus sham; $^\#P < 0.05$, $^{\#\#}P < 0.001$ versus Wt-cont; $^\dagger P < 0.01$, $^{\dagger\dagger}P < 0.001$ versus Wt-G ($n = 10$–15 for echocardiography and $n = 5$ for catheterization analysis). (d) Dose-dependent effects of G-CSF. FS, fractional shortening. $^*P < 0.01$ versus saline-treated mice (G-CSF = 0)($n = 12$–14). (e) Wild-type mice were operated to induce myocardial infarction and G-CSF treatment (100 μg/kg/d) was started from the indicated day for 5 d. $^*P < 0.05$, $^{**}P < 0.001$ versus saline-treated mice (C); $^\#P < 0.05$, $^{\#\#}P < 0.01$ versus mice treated at day 0 (d 0) ($n = 11$–12). (f) Effects of G-CSF on cardiac function at 1 week. $^*P < 0.05$ versus control ($n = 3$). (g) Effects of G-CSF on cardiac function of female mice. $^*P < 0.05$, $^{**}P < 0.001$ versus Wt-cont; $^\#P < 0.05$, $^{\#\#}P < 0.005$ versus Wt-G ($n = 4$–5).

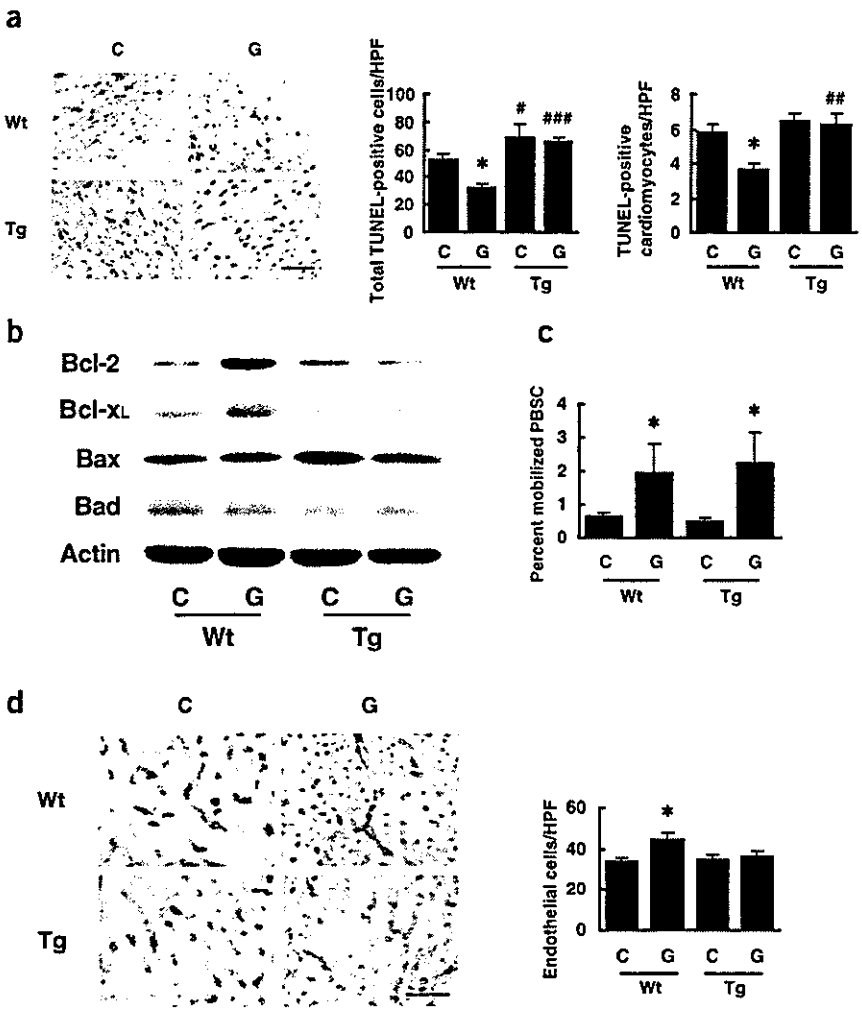

Figure 4 Mechanisms of the protective effects of G-CSF. (a) TUNEL staining (brown nuclei) in the infarcted hearts. The graphs show quantitative analyses for total TUNEL-positive cells (left graph) and TUNEL-positive cardiomyocytes (right graph) in infarcted hearts. $^{*}P < 0.01$ versus Wt-cont; $^{\#}P < 0.05$, $^{\#\#}P < 0.005$, $^{\#\#\#}P < 0.001$ versus wild-type mice with the same treatment ($n = 5$–7). Scale bar, 100 μm. (b) Infarcted hearts treated with G-CSF (G) or saline (C) were analyzed for expression of Bcl-2, Bcl-xL, Bax and Bad by western blotting ($n = 3$). (c) Mobilization of hematopoietic stem cells into peripheral blood (PBSC). $^{*}P < 0.05$ versus saline-treated mice ($n = 4$). (d) Capillary endothelial cells were identified by immunohistochemical staining with anti-PECAM antibody in the border zone of the infarcted hearts. Scale bar, 100 μm. The number of endothelial cells was counted and shown in the graph ($n = 6$–8). $^{*}P < 0.05$.

Mechanisms of the protective effects of G-CSF

Our *in vitro* results suggest that the protective effects of G-CSF on cardiac remodeling after myocardial infarction can be attributed in part to reduction of cardiomyocyte apoptosis. To determine whether the Stat3 pathway in cardiomyocytes mediates the antiapoptotic effects of G-CSF on the ischemic myocardium, we carried out TUNEL labeling of left ventricular sections 24 h after myocardial infarction in wild-type mice and dnStat3-Tg mice. Although the number of TUNEL-positive cells was significantly less in the Wt-G group than the Wt-cont group, G-CSF treatment had no effect on cardiomyocyte apoptosis in dnStat3-Tg mice (**Fig. 4a**). The effects of G-CSF on apoptosis after myocardial infarction were also attenuated when mice were treated with AG490 (**Supplementary Fig. 6** online). Myocardial infarction–related apoptosis was significantly increased in the Tg-cont group and AG490-treated wild-type mice compared with Wt-cont mice (**Fig. 4a** and **Supplementary Fig. 6** online), suggesting that endogenous activation of Stat3 has a protective role in the infarcted heart, as reported previously[25]. It is noteworthy that G-CSF treatment inhibited apoptosis of noncardiomyocytes including endothelial cells and that this inhibition was abolished in dnStat3-Tg mice (**Fig. 4a** and data not shown). To investigate the underlying molecular mechanism of the antiapoptotic effects of G-CSF *in vivo*, we examined expression of the Bcl-2 protein family by western blot analysis. Consistent with our *in vitro* results, expression of antiapoptotic proteins such as Bcl-2 and Bcl-xL was significantly increased in the Wt-G group at 24 h after myocardial infarction compared with the Wt-cont group, whereas expression of the proapoptotic proteins Bax and Bad was not affected by the treatment (**Fig. 4b**). In contrast, expression levels of antiapoptotic proteins were not increased by G-CSF in the Tg-G group (**Fig. 4b**). Immunohistochemical analysis also showed increased expression of Bcl-2 in the infarcted heart of the Wt-G group but not of the Tg-G group (**Supplementary Fig. 7** online).

To determine the effects of G-CSF on mobilization of stem cells, we counted the number of cells positive for both Sca-1 and c-kit in peripheral blood samples from mice treated with G-CSF or saline. The G-CSF treatment similarly increased the number of double-positive cells in wild-type mice and dnStat3-Tg mice (**Fig. 4c**). To examine the impact of G-CSF on cardiac homing of bone marrow cells, we transplanted bone marrow cells derived from GFP transgenic mice into wild-type and dnStat3-Tg mice, produced myocardial infarction and treated with G-CSF or saline. FACS analysis showed that G-CSF did not increase cardiac homing of bone marrow cells in wild-type and dnStat3-Tg mice (**Supplementary Fig. 8** online). We have shown that cardiac stem cells, which are able to differentiate into cardiomyocytes, exist in Sca-1-positive populations in the adult myocardium[26]. But G-CSF treatment did not affect the number of Sca-1-positive cells in the infarcted hearts of wild-type or dnStat3-Tg mice (**Supplementary Fig. 9** online). Thus, it is unlikely that G-CSF exerts its beneficial effects through expansion of cardiac stem cells. To determine the effects of G-CSF on proliferation of cardiomyocytes, we carried out immunostaining for Ki67, a marker for cell cycling, in conjunction with a labeling for troponin T. The number of Ki67-positive cardiomyocytes was increased in the infarcted hearts of wild-type mice and dnStat3-Tg mice compared with sham-operated mice (**Supplementary Fig. 10** online). But G-CSF did not alter the number of Ki67-positive cardiomyocytes in wild-type or dnStat3-Tg mice, suggesting that G-CSF does not induce proliferation of cardiomyocytes (**Supplementary Fig. 10** online). The number of Ki67-positive cardiomyocytes was less in infarcted hearts of dnStat3-Tg mice than in those of wild-type mice, suggesting that endogenous Stat3 activity is required

for myocardial regeneration after myocardial infarction and that activation of Stat3 by G-CSF is not sufficient for cardiomyocytes to enter the cell cycle in infarcted hearts of wild-type mice (**Supplementary Fig. 10** online). In contrast, G-CSF treatment significantly increased the number of endothelial cells in the border zone of the infarcted hearts (**Fig. 4d**). This increase was attenuated in dnStat3-Tg mice, indicating that the increased vascularity is mediated by Stat3 activity in cardiomyocytes and may partially account for the beneficial effects of G-CSF on the infarcted hearts. Taken together with the result that G-CSF-induced inhibition of noncardiomyocyte apoptosis was also mediated by the Stat3 signaling pathway in cardiomyocytes (**Fig. 4a**), these findings imply that communication between cardiomyocytes and noncardiomyocytes regulates each others' survival.

To further test whether G-CSF acts directly on the heart, we examined the effects of G-CSF treatment on cardiac function after ischemia-reperfusion injury in a Langendorff perfusion model. The isolated hearts underwent 30 min total ischemia followed by 120 min reperfusion with the perfusate containing G-CSF (300 ng/ml) or vehicle, and left ventricular developed pressure (LVDP, measured as the difference between systolic and diastolic pressures of the left ventricle) and LVEDP were measured. There were no significant differences in basal hemodynamic parameters including heart rate, left ventricular pressure, LVEDP and positive and negative dp/dt, between the control group and G-CSF group (**Table 1**). After reperfusion, however, G-CSF-treated hearts started to beat earlier than those of the control group (**Fig. 5a**). At 120 min after reperfusion, contractile function (LVDP) of G-CSF-treated hearts was significantly better than that of control hearts (**Fig. 5a**). Likewise, diastolic function (LVEDP) of G-CSF-treated hearts was better than that of control hearts (**Fig. 5a**). After ischemia-reperfusion, there was more viable myocardium (red lesion) in G-CSF-treated hearts than control hearts (**Fig. 5b**). The size of the infarct (white lesion) was significantly smaller in G-CSF-treated hearts than in control hearts (**Fig. 5b**).

Table 1 Basal hemodynamic parameters

	Control ($n = 7$)	G-CSF ($n = 7$)
HR (b.p.m.)	326 ± 34	334 ± 24
LVP (mmHg)	121.8 ± 24	117.3 ± 32
LVEDP (mmHg)	4.3 ± 1.3	4.5 ± 1.6
$+dp/dt$ (mmHg/s)	7,554 ± 643	7,657 ± 377
$-dp/dt$ (mmHg/s)	6,504 ± 638	6,670 ± 602

HR, heart rate; b.p.m., beats per minute; LVP, left ventricular pressure; LVEDP, left ventricular end-diastolic pressure; $+dp/dt$ and $-dp/dt$, positive and negative first derivatives for maximal rates of left ventricular pressure development.

DISCUSSION

In the present study, G-CSFR was found to be expressed on cardiomyocytes and cardiac fibroblasts, and G-CSF activated Jak2 and the downstream signaling molecule Stat3 in cultured cardiomyocytes. Treatment with G-CSF protected cultured cardiomyocytes from apoptotic cell death possibly through upregulation of Bcl-2 and Bcl-xL expression, suggesting that G-CSF has direct protective effects on cardiomyocytes through G-CSFR and the Jak-Stat pathway. This idea is further supported by the *in vivo* experiments. G-CSF enhanced Stat3 activity and increased expression of Bcl-2 and Bcl-xL in the infarcted heart where G-CSFR was markedly upregulated, thereby preventing cardiomyocyte apoptosis and cardiac dysfunction. These effects of G-CSF were abolished when Stat3 activation was disrupted in cardiomyocytes, suggesting that a direct action of G-CSF on cardiomyocytes has a crucial role in preventing left ventricular remodeling after myocardial infarction. Because noncardiomyocytes also expressed G-CSFR, the possibility exists that activation of G-CSF receptors on these cells modulates the beneficial effects of G-CSF on infarcted hearts.

The mobilization of bone marrow stem cells (BMSC) to the myocardium has been considered to be the main mechanism by which G-CSF ameliorates cardiac remodeling after myocardial infarction[1,6–8]. In this study, we showed that G-CSF reduces apoptotic cell death and effectively protects the infarcted heart, which is dependent on its direct action on cardiomyocytes through the Stat3 pathway. This antiapoptotic mechanism seems to be more important than induction of BMSC mobilization, because disruption of

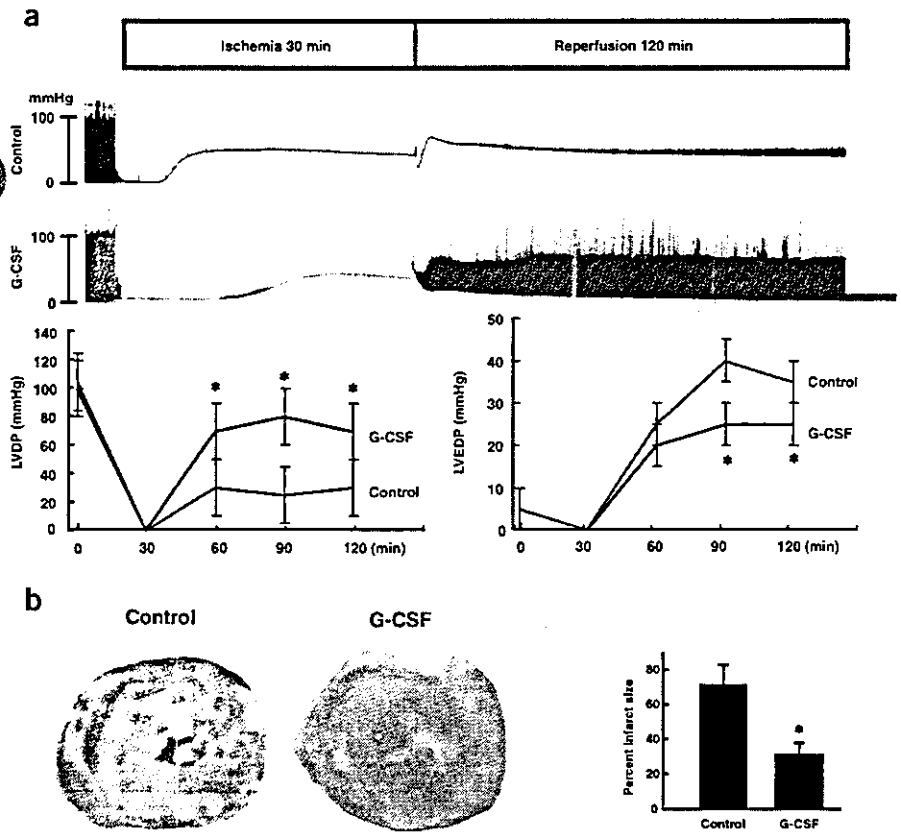

Figure 5 Direct effects of G-CSF on cardiac function after ischemia-reperfusion injury. (**a**) Representative left ventricular pressure records of control and G-CSF-treated hearts are shown (upper panel). The graphs show changes in LVDP (left) and LVEDP (right) during ischemia-reperfusion. $^*P < 0.05$ versus control hearts ($n = 7$). (**b**) The photographs show representative TTC staining of control hearts (Control) and G-CSF-treated hearts (G-CSF) after ischemia-reperfusion. The graph indicates myocardial infarct sizes for control hearts (Control) and G-CSF-treated hearts (G-CSF). Infarct sizes were calculated as described in **Supplementary Methods** online. $^*P < 0.05$ versus control hearts ($n = 7$).

this pathway by expressing dnStat3 in cardiomyocytes almost abolished the protective effects of G-CSF on cardiac remodeling after myocardial infarction. In addition, there was no difference in the effects of G-CSF on mobilization and cardiac homing of bone marrow cells, expansion of cardiac stem cells, and proliferation of cardiomyocytes between wild-type and dnStat3-Tg mice. The beneficial effects of G-CSF and stem cell factor on the infarcted heart has been described, but no evidence indicating that G-CSF induced cardiac homing of bone marrow cells in the infarcted heart has been shown[1]. In this study, we found favorable effects of G-CSF on the infarcted heart as early as 1 week after the treatment even though cardiac homing of bone marrow cells was not increased. Thus, we conclude that increased cardiac homing of bone marrow cells cannot account for improved function of the infarcted heart after G-CSF treatment.

The JAK-STAT pathway has been shown to induce various angiogenic factors besides antiapoptotic proteins[20,21]. The number of endothelial cells in the border zone was increased by G-CSF through Stat3 activation in cardiomyocytes. Consistent with this, we noted that G-CSF induces cardiac expression of angiogenic factors *in vitro* and *in vivo*, which appears to be mediated by cardiac Stat3 activation (M.H., Y.Q., H.T., T.M. & I.K., unpublished data). Moreover, we observed that the majority of apoptotic cells in the infarcted hearts was endothelial cells and that endothelial apoptosis was significantly inhibited by G-CSF treatment in wild-type mice but not in dnStat3-Tg mice (**Fig. 4a** and M.H., T.M. & I.K., unpublished data). Thus, activation of this pathway in cardiomyocytes by G-CSF may also promote angiogenesis and protect against endothelial apoptosis by producing angiogenic factors, resulting in the further prevention of cell death of cardiomyocytes and cardiac remodeling after myocardial infarction. The results in this study provide new mechanistic insights of the G-CSF therapy on infarcted hearts.

METHODS

For further details, please see **Supplementary Methods** online.

Cell culture. Cardiomyocytes prepared from ventricles of 1-d-old Wistar rats[27] were plated onto 60-mm plastic culture dishes at a concentration of 1×10^5 cells/cm^2 and cultured in Dulbecco modified Eagle medium (DMEM) supplemented with 10% fetal bovine serum (FBS) at 37 °C in a mixture of 95% air and 5% CO_2. The culture medium was changed to serum-free DMEM 24 h before stimulation. Generation and infection of recombinant adenovirus were performed as described[28].

Percoll enrichment of adult mouse cardiomyocytes and noncardiomyocytes. Adult mouse cardiomyocytes were prepared from 10-week-old C57BL/6 male mice according to the Alliance for Cellular Signaling protocol. We also prepared cardiomyocytes and noncardiomyocytes from myocardial infarction-operated or sham-operated C57BL/6 male mice. After digestion, cells were dissociated, resuspended in differentiation medium and loaded onto a discontinuous Percoll gradient. Cardiomyocytes or noncardiomyocytes were separately collected as described previously[29] and subsequently washed with 1 × phosphate-buffered saline for RT-PCR.

RNA extraction and RT-PCR analysis. Total RNA from adult mice cardiomyocytes was isolated by the guanidinium thiocyanate-phenol chloroform method. A total of 4 μg RNA was transcribed with MMLV reverse transcriptase and random hexamers. The cDNA was amplified using a mouse *Csf3r* exon 15 forward primer (5′-GTACTCTTGTCCACTACCTGT -3′) and an exon 17 reverse primer (5′-CAAGATACAAGGACCCCCAA -3′). We performed PCR under the following conditions: an initial denaturation at 94 °C for 2 min followed by a cycle of denaturation at 94 °C for 1 min, annealing at 58 °C for 1 min and extension at 72 °C for 1 min. We subjected samples to 40 cycles followed by a final extension at 72 °C for 3 min. The products were analyzed on a 1.5% ethidium bromide stained agarose gel.

Immunocytochemistry. Cardiomyocytes or noncardiomyocytes of neonatal rats cultured on glass cover slips were incubated with or without the antibody to G-CSFR (Santa Cruz Biotechnology) for 1 h, followed by incubation with Cy3-labeled secondary antibodies. After washing, we double-stained the cells with fluorescent phalloidin (Molecular Probes) for 1 h at room temperature.

Western blots. Western blot analysis was performed as described[5]. We probed the membranes with antibodies to phospho-Jak2, phospho-Stat3 (Cell Signaling), phospho-Jak1, phospho-Tyk2, phospho-Stat1, phospho-Stat5, anti-Jak1, Jak2, Tyk2, Stat1, Stat3, Stat5, Bcl-2, Bax, G-CSFR (Santa Cruz Biotechnology), Bcl-xL, Bad (Transduction Laboratories) or actin (Sigma-Aldrich). We used the ECL system (Amersham Biosciences Corp) for detection.

Animals and surgical procedures. Generation and genotyping of dnStat3-Tg mice have been previously described[28]. All mice used in this study were 8–10-week-old males, unless indicated. All experimental procedures were performed according to the guidelines established by Chiba University for experiments in animals and all protocols were approved by our institutional review board. We anesthetized mice by intraperitoneally injecting a mixture of 100 mg/kg ketamine and 5 mg/kg xylazine. Myocardial infarction was produced by ligation of the left anterior descending artery. We operated on dnStat3-Tg mice to induce myocardial infarction and randomly divided them into two groups, the G-CSF-treated group (10–100 μg/kg/d subcutaneously for 5 d consecutively, Kyowa Hakko Kogyo Co.) and the saline-treated group. We operated on nontransgenic mice as control groups using the same procedures and divided them into a G-CSF-treated group and a saline-treated group. Some mice were randomly chosen to be analyzed for initial area at risk by injection of Evans blue dye after producing myocardial infarction. There was no difference in initial area sizes at risk between saline-treated control and G-CSF-treated mice ($n = 5$; **Supplementary Fig. 11** online). We also determined initial infarct size by triphenyltetrazolium chloride staining on day 3. There was no significant difference in initial infarct size between saline-treated control and G-CSF-treated mice ($n = 5$; **Supplementary Fig. 12** online).

Echocardiography and catheterization. Transthoracic echocardiography was performed with an Agilent Sonos 4500 (Agilent Technology Co.) provided with an 11-MHz imaging transducer. For catheterization analysis, the right carotid artery was cannulated under anesthesia by the micro pressure transducers with an outer diameter of 0.42 mm (Samba 3000; Samba Sensors AB), which was then advanced into the left ventricle. Pressure signals were recorded using a MacLab 3.6/s data acquisition system (AD Instruments) with a sampling rate of 2,000 Hz. Mice were anesthetized as described above, and heart rate was kept at approximately 270–300 beats per minute to minimize data deviation when we measured cardiac function.

Histology. Hearts fixed in 10% formalin were embedded in paraffin, sectioned at 4 μm thickness, and stained with Masson trichrome. The extent of fibrosis was measured in three sections from each heart and the value was expressed as the ratio of Masson trichrome stained area to total left ventricular free wall. For apoptosis analysis, infarcted hearts were frozen in cryomolds, sectioned, and TUNEL labeling was performed according to the manufacturer's protocol (*In Situ* Apoptosis Detection kit; Takara) in combination with immunostainings for appropriate cell markers. Digital photographs were taken at magnification ×400, and 25 random high-power fields (HPF) from each heart sample were chosen and quantified in a blinded manner. We examined vascularization by measuring the number of capillary endothelial cells in light-microscopic sections taken from the border zone of the hearts 2 weeks after myocardial infarction. Capillary endothelial cells were identified by immunohistochemical staining with antibody to platelet endothelial cell adhesion molecule (PECAM; Pharmingen). Ten random microscopic fields in the border zone were examined and the number of endothelial cells was expressed as the number of PECAM-positive cells/HPF (magnification, ×400).

Statistical analysis. Data are shown as mean ± s.e.m. Multiple group comparison was performed by one-way analysis of variance (ANOVA) followed by the Bonferroni procedure for comparison of means. Comparison between two groups were analyzed by the two-tailed Student's *t*-test or two-way ANOVA. Values of $P < 0.05$ were considered statistically significant.

URL. Alliance for Cellular Signaling Procedure Protocols
http://www.signaling-gateway.org/data/cgi-bin/Protocols.cgi?cat=0

Note: Supplementary information is available on the Nature Medicine website.

ACKNOWLEDGMENTS

The authors thank J. Robbins (Children's Hospital Research Foundation, Cincinnati, Ohio) for a fragment of the αMHC gene promoter, M. Tamagawa for the analysis of Langendorff-perfused model, Kirin Brewery Co., Ltd. for their kind gift of G-CSF, and M. Watanabe and E. Fujita for their technical assistance. This work was supported by a Grant-in-Aid for Scientific Research, Developmental Scientific Research, and Scientific Research on Priority Areas from the Ministry of Education, Science, Sports, and Culture and by the Program for Promotion of Fundamental Studies in Health Sciences of the Organization for Drug ADR Relief, R&D Promotion and Product Review of Japan (to I.K.) and Japan Research Foundation for Clinical Pharmacology (to T.M.).

COMPETING INTERESTS STATEMENTS

The authors declare that they have no competing financial interests.

Received 8 September 2004; accepted 19 January 2005
Published online at http://www.nature.com/naturemedicine/

1. Orlic, D. *et al.* Mobilized bone marrow cells repair the infarcted heart, improving function and survival. *Proc. Natl. Acad. Sci. USA* **98**, 10344–10349 (2001).
2. Ohtsuka, M. *et al.* Cytokine therapy prevents left ventricular remodeling and dysfunction after myocardial infarction through neovascularization. *FASEB J.* **18**, 851–853 (2004).
3. Moon, C. *et al.* Erythropoietin reduces myocardial infarction and left ventricular functional decline after coronary artery ligation in rats. *Proc. Natl. Acad. Sci. USA* **100**, 11612–11617 (2003).
4. Parsa, C.J. *et al.* A novel protective effect of erythropoietin in the infarcted heart. *J. Clin. Invest.* **112**, 999–1007 (2003).
5. Zou, Y. *et al.* Leukemia inhibitory factor enhances survival of cardiomyocytes and induces regeneration of myocardium after myocardial infarction. *Circulation* **108**, 748–753 (2003).
6. Minatoguchi, S. *et al.* Acceleration of the healing process and myocardial regeneration may be important as a mechanism of improvement of cardiac function and remodeling by postinfarction granulocyte colony-stimulating factor treatment. *Circulation* **109**, 2572–2580 (2004).
7. Adachi, Y. *et al.* G-CSF treatment increases side population cell infiltration after myocardial infarction in mice. *J. Mol. Cell. Cardiol.* **36**, 707–710 (2004).
8. Kawada, H. *et al.* Nonhematopoietic mesenchymal stem cells can be mobilized and differentiate into cardiomyocytes after myocardial infarction. *Blood* **104**, 3581–3587 (2004).
9. Avalos, B.R. Molecular analysis of the granulocyte colony-stimulating factor receptor. *Blood* **88**, 761–777 (1996).
10. Demetri, G.D. & Griffin, J.D. Granulocyte colony-stimulating factor and its receptor. *Blood* **78**, 2791–808 (1991).
11. Berliner, N. *et al.* Granulocyte colony-stimulating factor induction of normal human bone marrow progenitors results in neutrophil-specific gene expression. *Blood* **85**, 799–803 (1995).
12. Orlic, D. *et al.* Bone marrow cells regenerate infarcted myocardium. *Nature* **410**, 701–705 (2001).
13. Asahara, T. *et al.* Bone marrow origin of endothelial progenitor cells responsible for postnatal vasculogenesis in physiological and pathological neovascularization. *Circ. Res.* **85**, 221–228 (1999).
14. Kocher, A.A. *et al.* Neovascularization of ischemic myocardium by human bone-marrow-derived angioblasts prevents cardiomyocyte apoptosis, reduces remodeling and improves cardiac function. *Nat. Med.* **7**, 430–436 (2001).
15. Jackson, K.A. *et al.* Regeneration of ischemic cardiac muscle and vascular endothelium by adult stem cells. *J. Clin. Invest.* **107**, 1395–1402 (2001).
16. Balsam, L.B. *et al.* Haematopoietic stem cells adopt mature haematopoietic fates in ischaemic myocardium. *Nature* **428**, 668–673 (2004).
17. Murry, C.E. *et al.* Haematopoietic stem cells do not transdifferentiate into cardiac myocytes in myocardial infarcts. *Nature* **428**, 664–668 (2004).
18. Norol, F. *et al.* Influence of mobilized stem cells on myocardial infarct repair in a nonhuman primate model. *Blood* **102**, 4361–4368 (2003).
19. Aarts, L.H., Roovers, O., Ward, A.C. & Touw, I.P. Receptor activation and 2 distinct COOH-terminal motifs control G-CSF receptor distribution and internalization kinetics. *Blood* **103**, 571–579 (2004).
20. Benekli, M., Baer, M.R., Baumann, H. & Wetzler, M. Signal transducer and activator of transcription proteins in leukemias. *Blood* **101**, 2940–2954 (2003).
21. Smithgall, T.E. *et al.* Control of myeloid differentiation and survival by Stats. *Oncogene* **19**, 2612–2618 (2000).
22. Dumont, E.A. *et al.* Cardiomyocyte death induced by myocardial ischemia and reperfusion: measurement with recombinant human annexin-V in a mouse model. *Circulation* **102**, 1564–1568 (2000).
23. van Heerde, W.L. *et al.* Markers of apoptosis in cardiovascular tissues: focus on Annexin V. *Cardiovasc. Res.* **45**, 549–559 (2000).
24. Bromberg, J. Stat proteins and oncogenesis. *J. Clin. Invest.* **109**, 1139–1142 (2002).
25. El-Adawi, H. *et al.* The functional role of the JAK-STAT pathway in post-infarction remodeling. *Cardiovasc. Res.* **57**, 129–138 (2003).
26. Matsuura, K. *et al.* Adult cardiac Sca-1-positive cells differentiate into beating cardiomyocytes. *J. Biol. Chem.* **279**, 11384–11391 (2004).
27. Zou, Y. *et al.* Both Gs and Gi proteins are critically involved in isoproterenol-induced cardiomyocyte hypertrophy. *J. Biol. Chem.* **274**, 9760–9770 (1999).
28. Funamoto, M. *et al.* Signal transducer and activator of transcription 3 is required for glycoprotein 130-mediated induction of vascular endothelial growth factor in cardiac myocytes. *J. Biol. Chem.* **275**, 10561–10566 (2000).
29. Ikeda, K. *et al.* The effects of sarpogrelate on cardiomyocyte hypertrophy. *Life Sci.* **67**, 2991–2996 (2000).

ELSEVIER

European Journal of Cardio-thoracic Surgery 26 (2004) 1174–1179

EUROPEAN JOURNAL OF CARDIO-THORACIC SURGERY

www.elsevier.com/locate/ejcts

Residual fibrosis affects a long-term result of left ventricular volume reduction surgery for dilated cardiomyopathy in a rat experimental study☆

Taiko Horii[a,b], Keiichi Tambara[a], Kazunobu Nishimura[a], Hisayoshi Suma[b], Masashi Komeda[a,*]

[a]*Department of Cardiovascular Surgery, Graduate school of Medicine, Kyoto University, Kyoto, Japan*
[b]*Hayama Heart Center, Hayama, Japan*

Received 18 November 2003; received in revised form 11 June 2004; accepted 16 June 2004; Available online 11 September 2004

Abstract

Objectives: The aim of this study is to evaluate the relationship between left ventricular (LV) wall property and the results of LV volume reduction surgery (LVR) to treat dilated cardiomyopathy (DCM) in an experimental model. **Methods**: DCM was introduced in 18 Lewis rats by autoimmunization with cardiac myosin. Among them, 12 rats underwent LVR and the rest were served as controls. They were subjected to echocardiography and cardiac catheterization for dimensional and functional measurements. The animals were sacrificed 4 weeks after surgery, and the fraction of myocardial fibrosis was calculated in 4 divided parts of the LV wall. **Results**: Percent fibrosis varied widely from 4.7 to 45.2%. LV volume reduction surgery improved cardiac function immediately after surgery in all rats (E_{max}, 0.28±0.14 to 0.48±0.18 mmHg/μl; LV end-diastolic pressure, 21.0±6.1 to 13.3±5.1 mmHg, $P<0.05$, respectively). Four weeks later, 6 hearts remained in good shape with smaller LV end-diastolic dimension (Dd) than baseline values (LV Dd, 9.7±0.6 mm; fractional area change (FAC), 40.3±8.4%) and the other 6 had more redilation in diameter and more deterioration in function than baseline values (LV Dd, 10.9±0.6 mm; FAC, 25.8±6.9%; $P<0.05$, respectively). Percent fibrosis in the septum differed 11.1±3.4 vs. 27.8±2.8% between the two groups ($P<0.01$). There was a significant correlation between the ratio of LV redilatation after surgery and percent fibrosis in the septum ($r=0.951$, $P<0.01$). **Conclusions**: Although the initial benefit of LVR was confirmed, the long-term result was affected by the amount of residual fibrosis. This information suggests that surgical site selection is important to achieve a good result of LV restoration surgery for DCM.

Keywords: Dilated cardiomyopathy; Heart failure; Left ventricular restoration

1. Introduction

Initial enthusiasm of partial left ventriculectomy (PLV), so called Batista operation, to treat dilated cardiomyopathy (DCM) has quickly diminished partially due to an unpredictable mid-term result [1,2]

PLV works very well in some patients, but not so well or even worse in others. The reason why the effect of PLV is inconsistent remains unclear so far.

In our clinical practice, we noticed that the left ventricle of DCM was not always homogeneously affected as pointed out previously [3,4]. Some patients have inhomogeneous left ventricular (LV) wall property, and others have diffusely and homogeneously damaged LV wall [5,6].

The hypothesis is that the surgical benefit does not last long if fibrosis was prominent in the retained myocardium after PLV. The main purpose of PLV is to reduce the diameter and the volume of the left ventricle, and therefore we perform LV volume reduction surgery (LVR) as an alternative to PLV in this study. We have focused attention to the LV wall property as assessed by the amount of myocardial fibrosis and evaluated the relationship between the residual fibrosis of the retained myocardium and the surgical result of LV volume reduction surgery in a rat DCM model.

2. Materials and methods

2.1. Animal information

Young male Lewis rats were used in this study.

☆ Presented at the joint 17th Annual Meeting of the European Association for Cardio-thoracic Surgery and the 11th Annual Meeting of the European Society of Thoracic Surgeons, Vienna, Austria, October 12–15, 2003.

*Corresponding author. Tel.: +81 75 751 3781; fax: +81 75 751 3098.
E-mail address: masakom@kuhp.kyoto-u.ac.jp (M. Komeda).

1010-7940/$ - see front matter © 2004 Published by Elsevier B.V.
doi:10.1016/j.ejcts.2004.06.023

All animals received humane care in compliance with Principles of Laboratory Animal Care formulated by the National Society for Medical Research and the Guide for the Care and Use of Laboratory Animals prepared by the Institute Council and published by the National Academy Press.

2.2. DCM model

Six weeks old Lewis rats were autoimmunized with purified cardiac myosin and later on developed DCM as reported elsewhere [7,8]. Animals have suffered from sort of acute myocarditis for 4–5 weeks and such inflammatory reaction almost disappeared within 8 weeks after autoimmunization [9].

Ten weeks after autoimmunization all animals were evaluated by means of echocardiography. Rats with dilated LV and severely depressed LV function confirmed by echocardiography were provided for this study. After all, 18 rats completed the study, among which 12 rats underwent surgical intervention and the rest were served as controls.

2.3. Echocardiographic study

Rats were anesthetized with ether and LV function was assessed by means of echocardiography with a 12 MHz phased-array transducer (SONOS 5500, Philips Medical Systems, Bothell, WA, USA) [10–12]. The following parameters were measured from B- and M-mode tracing: LV end-diastolic dimension (LV Dd, mm), LV end-systolic dimension (LV Ds, mm), fractional shortening (FS, %), and fractional area change (FAC, %). All parameters were measured by the American Society for Echocardiography leading-edge method from at least three consecutive cardiac cycles.

Echocardiography was performed before and immediately after surgery, following 2 and 4 weeks after surgery serially.

2.4. LV volume reduction surgery

Animals were orally intubated with ethyl ether gas and anesthesia was maintained with 1% isoflurane under control ventilation during operation. LV volume reduction surgery (LVR) was carried out by placation of the posterolateral wall. LV was gently pulled out from the pericardial cavity via left thoracotomy and the posterolateral wall of the left ventricle was plicated with several horizontal mattress sutures of 4-0 prolene without any kind of cardiac support. Surgical technique performed in this study was similar with the technique adapted to a large animal model, apex-preserving LVR [13]. Before and after surgery, echocardiography and cardiac catheterization were performed simultaneously and the efficacy of the surgical technique was evaluated.

2.5. Cardiac catheterization

A 2 French micromanometer-tipped catheter (Millar Instruments Inc, Houston, TX) was introduced from the right carotid artery to measure LV pressure and a 3 French occlusion balloon catheter was introduced from the right femoral vein to occlude the inferior vena cava. At the stable state, LV pressure and its first time derivative (dp/dt) were continuously monitored through the arterial catheter by using a multiple recording system during temporary caval occlusion. Simultaneously LV dimension was measured by echocardiography. The maximum time-varying elastance (LV E_{max}, mmHg/μl) and the time constant of isovolumic relaxation (Tau τ, ms) was calculated as an index of global systolic and diastolic function, respectively [10–12].

2.6. Histological study

At 4 weeks after surgery, final echocardiography was performed and all rats were sacrificed. Hearts were removed and transected at the base of the papillary muscles. The transverse sections were fixed with 10% formalin and stained with hematoxylin eosin and Masson's trichrome staining. In the same manner six DCM rats without LVR were served as control group.

The heart sections were divided into four parts: anterior, septal, posterior, and lateral part. Masson's trichrome stained sections were subjected to quantitative evaluation of the severity of interstitial fibrosis (percent fibrosis) using the point counting method.

2.7. Statistical analysis

Data were expressed as means ± SD. Statistical analysis was performed by using StatView (SAS Institute Inc, Cary, NC). Differences between two groups were assessed by the non-parametric test, Wilcoxon test and Mann–Whitney U-test. Correlation trends were assessed by Spearman rank correlation coefficient r. Values of P less than 0.05 were considered statistically significant.

3. Result

3.1. Echocardiography at baseline

Sixty-eight rats out of 100 rats which were autoimmunized with cardiac myosin survived until echocardiographic study at 8 weeks after initial manipulation. Fifty-two rats were diagnosed as DCM by echocardiography. The reasons of exclusion were as follows: LV cavity was not enough enlarged, LV wall motion was too much depressed (i.e. almost dying), or right ventricle was also severely enlarged or depressed.

Table 1 summarized echocardiographic data at baseline. LV Dd and LV Ds of DCM rats became bigger than those

Table 1
Echocardiographic data in control and DCM group

Variable	DCM ($n=12$)	Normal ($n=7$)	P-value
LV Dd (mm)	10.1±0.6	7.6±0.3	<0.001
LV Ds (mm)	7.8±0.7	3.3±0.2	<0.001
FS (%)	23.1±3.4	55.4±2.2	<0.001
FAC (%)	31.6±4.5	82.1±7.9	<0.001

Data are expressed as mean±SD. LV Dd, left ventricular end-diastolic dimension; LV Ds, left ventricular end-systolic dimension; FAC, fractional area change; FS, fractional shortening.

of health Lewis rats of the same age (normal control). FS and FAC of DCM rats were lower than those of normal control.

DCM rats had significantly larger hearts and poorer LV function than normal control group.

3.2. Cardiac catheterization before and after surgery

E_{max} and the maximal LV dp/dt increased after surgery. The LV end-diastolic pressure, minimum LV dp/dt, and τ decreased after surgery. The values measured by the catheterization were summarized in Table 2 and there was a significant difference between values before and after surgery.

Systolic function of LV improved after surgery without compromising diastolic function. In addition, the surgical technique used in the present study avoided excessive volume reduction of the left ventricle.

3.3. Serial echocardiographic change after surgery

Thirty-five rats underwent LV volume reduction surgery and 24 rats survived surgery. In 16 rats LVR was properly carried out and the efficacy of the surgery was confirmed by echocardiography and cardiac catheterization. Among them, 12 rats survived 4 weeks after surgery and were subjected to serial echocardiographic follow-up completely.

Comparing LV dimensions at 4 weeks after surgery with those at baseline, rats were divided into two groups as follows. One was Good result group, of which LV dimension at 4 weeks after surgery remained smaller than that at baseline. The other was Poor result group, of which LV dimension at 4 weeks after surgery became larger than that at baseline. LV Dd of Poor result group increased quicker and more severely than that of Good result group, as shown in Fig. 1.

Table 2
Cardiac catheterization data before and after surgery

	Pre	Post	P-value
LVEDP (mmHg)	21.0±6.1	13.3±5.1	<0.05
E_{max} (mmHg/μl)	0.28±0.14	0.48±0.18	<0.05
+LV dp/dt (mmHg/s)	3583±559	4430±724	<0.05
−LV dp/dt (mmHg)	−2385±196	−2797±507	<0.05
Tau τ (ms)	36.6±8.4	29.3±7.4	<0.05

Data are expressed as mean±SD. LVEDP, left ventricular end-diastolic pressure; LV E_{max}, maximal time-varying elastance; +LV dp/dt, maximal time-derivative; −LV dp/dt, minimal time-derivative; Tau τ, time constant of isovolumetric relaxation.

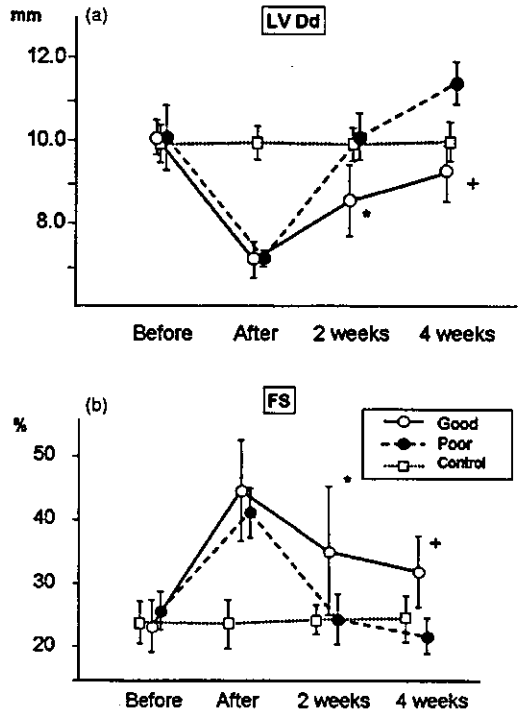

Fig. 1. (A) and (B) Serial echocardiographic change of cardiac function after surgery. (A) Change of left ventricular end-diastolic dimension (LV Dd): LV dimension once reduced by surgery increased time by time. LV redilatation of Bad result group was much more intense than that of Good result group. (B) Change of fractional shortening (FS): LV function once improved by surgery deteriorated time by time. LV function of Bad result group was more deteriorated than that of Good result group. $^{*}P<0.05$, $^{+}P<0.001$ vs. Poor group.

The dimension of the left ventricle was uniformly reduced by surgery, following progressive redilatation time by time. LV Dd and LV Ds in Poor result group increased more quickly and severely than those in Good result group, as shown in Table 3 and Fig. 1. Similarly, FS and FAC of LV increased uniformly after surgery in both groups, following progressive deterioration time by time. FS and FAC of Poor result group deteriorated quicker and more severely than those of Good result group as shown in Table 3.

3.4. Histological study

3.4.1. Control DCM rats

Fractional fibrosis calculated as percent fibrosis varied widely from 4.4 to 45.2% part by part and localization of fibrosis varied. In the present model of DCM, fibrosis scattered around and localization of fibrosis differed rats by rats as shown in Table 4. The most fibrotic parts of each individual hearts differed rats by rats. The anterior part was the most fibrotic in one of 6 rats, the septum in 2, the posterior in one, and the lateral in 2. The anteroseptal wall

Table 3
Serial echocardiographic change after surgery

	Group	Pre	Post	2 Weeks	4 Weeks
LV Dd (mm)	Good	10.1±0.4	7.1±0.4	8.6±0.9*	9.7±0.6^{+}
	Poor	10.1±±0.8	7.2±0.2	10.2±0.6	10.9±0.6
LV Ds (mm)	Good	7.8±0.6	4.0±0.8	5.8±0.7^{+}	6.4±0.7^{+}
	Poor	7.8±0.8	4.4±0.4	8.0±0.8	9.1±0.7
FS (%)	Good	23.2±4.1	44.6±7.9	35.1±10.1*	33.9±6.1^{+}
	Poor	23.2±3.0	38.7±3.9	21.9±4.1	16.2±3.0
FAC (%)	Good	33.6±5.1	50.2±7.1	43.6±9.6	40.0±8.4^{+}
	Poor	31.6±4.5	47.0±5.8	32.1±9.2	25.8±6.9

Data are expressed as mean±SD. Pre, before surgery; Post, 4 weeks after surgery; Good, Good result group; Poor, Poor result group; LV Dd, left ventricular end-diastolic dimension; LV Ds, left ventricular end-systolic dimension; FS, fractional shortening; FAC, fractional area change. *$P<0.05$, $^{+}P<0.001$ vs. Poor group

was more fibrotic than posterolateral wall in 3 of 6 rats and the posterolateral wall was more fibrotic than the anteroseptal wall in 3. The LV wall of the DCM rats was not homogeneously damaged as shown in Fig. 2.

3.4.2. Four weeks after surgery

Percent fibrosis of the septum, which was far from surgical site and presumably least damaged by surgery itself, in Good result group was significantly smaller than that in Poor result group (11.3±3.4 vs. 27.8±2.8%, $P<0.0001$). Regarding percent fibrosis of the rest of the heart, which consisted of the anterior part and the posterior part, there was no big difference between both groups (14.9±4.9 vs. 22.7±8.1%, $P=0.07$).

Comparing the relationship between the ratio of LV redilatation (delta redilatation) and percent fibrosis of the septum, there was a strong correlation recognized between them ($r=0.951$, $P<0.001$) as shown in Fig. 3.

The ratio of LV redilatation was calculated as follows; (LV Dd after−LV Dd before)/LV Dd before×100 (%).

4. Discussion

Dr Batista introduced the surgical concept of resecting sound muscle and reducing LV diameter in order to improve LV function of enlarged DCM hearts according to the physics [14]. This concept seemed attractive to treat end-stage heart failure and brought broad attention not only to the surgical community but also to the entire cardiovascular medicine. A short-term result of PLV to treat a difficult patient group of end-stage heart failure was good enough to convince many surgeons to start performing PLV. However, unpredictable and inconsistent mid-term results have gradually been revealed and the initial hope to PLV has diminished quickly [1,2].

In 1996 we started performing PLV for DCM and achieved good initial results, following unpredictable mid-term result as occurred similarly around the world. We examined LV wall motion thoroughly by echocardiography with utilizing color kinetic method before surgery and intraoperatively and we noticed some patients had abnormal regional wall motion [5,6]. Abnormal LV wall motion and heterogeneity of LV wall property in DCM was pointed out previously [3,4]. According to the echocardiographic findings, we started SAVE operation, septal anterior ventricular exclusion, instead of PLV when LV wall motion of the anteroseptal part was worse than that of the posterolateral part [15,16]. Then left ventriculoplasty for DCM by careful selection of PLV and SAVE improved a mid-tem result. Four year survival rate of 61 elective operations was 69.3% [17].

Table 4
Histological data of control DCM rats

Part	% Fibrosis	%
Anterior	17.5±14.0	6.9–45.2
Septum	15.4±9.8	4.7–49.8
Posterior	12.3±5.3	4.4–18.1
Lateral	19.7±10.9	7.6–35.1
Total	16.2±10.2	4.4–45.2

Data are expressed as mean±SD. Part, each four divided part of the heart in the transverse section.

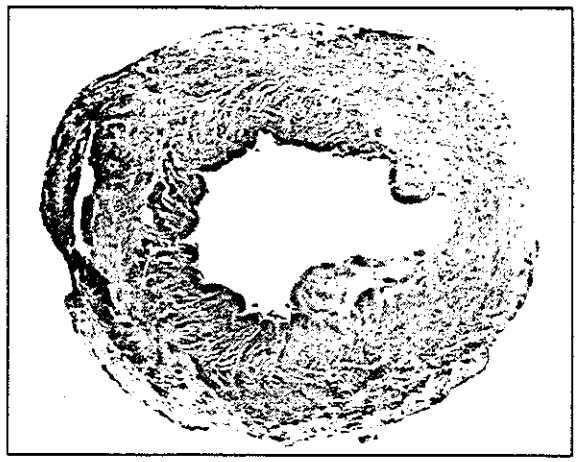

Fig. 2. Masson's trichrome staining of transected LV. In this specimen, fibrosis distributes prominently in the lateral wall. The lateral wall is more fibrotic than the anteroseptal wall. Fibrosis is not diffusely scattered and localized in the lateral wall.

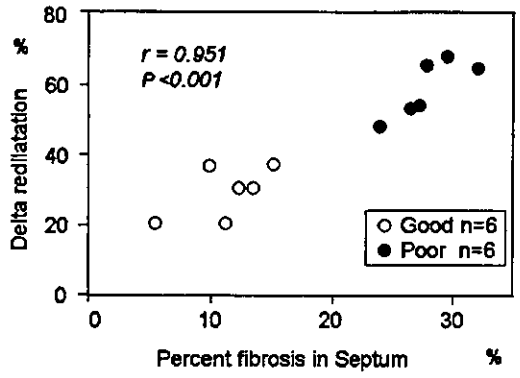

Fig. 3. The relationship between the ratio of LV redilatation and the fractional fibrosis in the septum. The more dilated LV dimension became after surgery, the more fibrotic the septum retained by surgery was. Delta redilatation was explained in the text.

In the present study, we adopted a DCM model created by means of autoimmunization with cardiac myosin because this model type is mimicked with humane DCM without hypertension [7,8]. Histological study showed that localized fibrosis scattered in the left ventricle and location of fibrosis differed individually. This means that the LV wall in this DCM model has inhomogeneous histology, and that the model is suitable for evaluating the relationship between LV wall property and the surgical result.

The findings of the present study are summarized as follows. Echocardiography and cardiac catheterization confirmed the efficacy of the surgery, but LV diameter which had been reduced right after the surgery had gradually enlarged as time passed. The ratio of LV redilatation differed in two groups. Half of animals remained in good shape with smaller LV dimension than baseline, and the other half deteriorated in bad shape with larger LV dimension. Histological study showed the fraction of residual fibrosis in Good result group was significantly less than that in Bad result group. There was a strong correlation between the ratio of LV redilatation and the relative amount of residual fibrosis.

This study infers that localization of fibrosis affects the long-term result of PLV. Decreasing number of heart transplantation around the world, there seeks a possibility of non-transplant surgery for end-stage heart failure. Initial experience of PLV has left a fact that PLV could salvage some candidates for heart transplantation to a considerable extent in spite of denying the almightiness of PLV [2]. We must consider not only resecting the posterolateral wall like PLV but also some intervention to the anteroseptal wall such as SAVE operation depending on the patients' LV wall property. Such a strategic approach as a combination of resecting damaged myocardium and retaining sound muscle can improve a long-term result of LV restoration surgery for DCM.

In conclusion, a long-term result of LV volume reduction surgery for DCM rats was affected by the amount of residual fibrosis. This information suggests that proper selection of the surgical site is important to achieve a good result of LV restoration surgery for DCM.

5. Study limitations

This study was conducted as a retrospective analysis to examine the result of the surgery. We can conduct the study prospectively if we recognized the LV wall property exactly before surgery. In the present time we have no reliable tool to examine the interstitial fibrosis of the whole heart without excising the heart for pathological examinations. Alternatively we sacrificed 6 DCM rats before surgery for histological study, which confirmed that they had wide variety of LV wall property in terms of myocardial fibrosis.

Further development of the technology may help to detect the LV wall property exactly and predict the result of the surgery prospectively.

References

[1] Gorcsan 3rd J, Feldman AM, Kormos RL, Mandarino WA, Demetris AJ, Batista RJ. Heterogeneous immediate effects of partial left ventriculectomy on cardiac performance. Circulation 1998;97: 839–42.

[2] Franco-Cereceda A, McCarthy PM, Blackstone EH, Hoercher KJ, White JA, Young JB, Starling RC. Partial left ventriculectomy for dilated cardiomyopathy: is this an alternative to transplantation? J Thorac Cardiovasc Surg 2001;121:879–93.

[3] Bach DS, Beanlands RS, Schwaiger M, Armstrong WF. Heterogeneity of ventricular function and myocardial oxidative metabolism in nonischemic dilated cardiomyopathy. J Am Coll Cardiol 1995;25: 1258–62.

[4] Young AA, Dokos S, Powell KA, Sturm B, McCulloch AD, Starling RC, McCarthy PM, White RD. Regional heterogeneity of function in nonischemic dilated cardiomyopathy. Cardiovasc Res 2001;49:308–18.

[5] Suma H, Isomura T, Horii T, Sato T, Kikuchi N, Iwahashi K, Hosokawa J. Nontransplant cardiac surgery for end-stage cardiomyopathy. J Thorac Cardiovasc Surg 2000;119:1233–44.

[6] Isomura T, Suma H, Horii T, Sato T, Kikuchi N. Partial left ventriculectomy, ventriculoplasty or valvular surgery for idiopathic dilated cardiomyopathy—the role of intra-operative echocardiography. Eur J Cardiothorac Surg 2000;17:239–45.

[7] Kodama M, Hanawa H, Saeki M, Hosono H, Inomata T, Suzuki K, Shibata A. Rat dilated cardiomyopathy after autoimmune giant cell myocarditis. Circ Res 1994;75:278–84.

[8] Hirono S, Islam MO, Nakazawa M, Yoshida Y, Kodama M, Shibata A, Izumi T, Imai S. Expression of inducible nitric oxide synthase in rat experimental autoimmune myocarditis with special reference to changes in cardiac hemodynamics. Circ Res. 1997;80: 11–20.

[9] Okura Y, Yamamoto T, Goto S, Inomata T, Hirono S, Hanawa H, Feng L, Wilson CB, Kihaya I, Izumi T, Shibata A, Aizawa Y, Seki S, Abo T. Characterization of cytokine and iNOS mRNA expression in situ during the course of experimental autoimmune myocarditis in rats. J Mol Cell Cardiol 1997;29:491–502.

[10] Nishina T, Nishimura K, Yuasa S, Miwa S, Nomoto T, Sakakibara Y, Handa N, Hamanaka I, Saito Y, Komeda M. Initial effects of the left ventricular repair by plication may not last long in a rat ischemic cardiomyopathy model. Circulation 2001;104:I241–I245.
[11] Sakakibara Y, Tambara K, Lu F, Nishina T, Nagaya N, Nishimura K, Komeda M. Cardiomyocyte transplantation does not reverse cardiac remodeling in rats with chronic myocardial infarction. Ann Thorac Surg 2002;74:25–30.
[12] Tambara K, Sakakibara Y, Sakaguchi G, Lu F, Premarantne GU, Lin X, Nishimura K, Komeda M. Transplanted skeletal myoblasts can fully replace the infracted myocardium when they survive in the host in large numbers. Circulation 2003;108:II259–II263.
[13] Koyama T, Nishimura K, Unimonh O, Ueyama A, Komeda M. Importance of preserving the apex and plication of the base in left ventricular volume reduction surgery. J Thorac Cardiovasc Surg 2003; 125:669–77.
[14] Batista RJ, Santos JL, Takeshita N, Bocchino L, Lima PN, Cunha MA. Partial left ventriculectomy to improve left ventricular function in end-stage heart disease. J Card Surg 1996;11:96–7 (discussion 98).
[15] Suma H. Internal left ventricular reconstruction. Op Techs Thorac Cardiovasc Surg 2001;13:514–21.
[16] Isomura T, Suma H, Horii T, Sato T, Kobashi T, Kanemitsu H, Hoshino J, Hisatomi K. Left ventricle restoration in patients with non-ischemic dilated cardiomyopathy: risk factors and predictors of outcome and change of mid-term ventricular function. Eur J Cardiothorac Surg 2001;19:684–9.
[17] Horii T, Isomura T, Komeda M, Suma H. Left ventriculoplasty for nonischemic dilated cardiomyopathy. J Card Surg 2003;18:121–4.

Appendix A. Conference discussion

Dr R. Poston (Baltimore, MD, USA): The hearts that did bad, did they have more overall inflammation, or was it localized to the septum?

Dr Horii: I don't follow you.

Dr Poston: It is possible that there is just overall more myocardial inflammation and fibrosis that also included the septum in the hearts that did bad which was not necessarily specific to the septum. If that's the case, it could just be that in your model a bad heart outcome is due mainly to a more intense inflammatory response from the autoimmune stimulus. Irregardless of the ventricular surgery, the inflammatory response led to the hearts dilating back out.

Dr Horii: Unfortunately, I don't have a good answer for you, because I cannot tell you if such a fibrosis is the reason or is the cause.

Regarding myocardial fibrosis, the septum was the least damaged by surgery itself and the least fibrotic portion as shown in my presentation. And even in the clinical setting and also in this experimental setting, there was localized fibrosis and heterogeneity of LV wall in DCM hearts. And so, LV surgery can be performed in an appropriate way to treat DCM hearts.

Journal of the American College of Cardiology
© 2004 by the American College of Cardiology Foundation
Published by Elsevier Inc.

Vol. 44, No. 7, 2004
ISSN 0735-1097/04/$30.00
doi:10.1016/j.jacc.2004.07.017

Surgical Ventricular Restoration in the Treatment of Congestive Heart Failure Due to Post-Infarction Ventricular Dilation

Constantine L. Athanasuleas, MD,* Gerald D. Buckberg, MD,† Alfred W. H. Stanley, MD,* William Siler, PHD,* Vincent Dor, MD,‡ Marisa Di Donato, MD,§ Lorenzo Menicanti, MD,‖ Sergio Almeida de Oliveira, MD,¶ Friedhelm Beyersdorf, MD,# Irving L. Kron, MD,** Hisayoshi Suma, MD,†† Nicholas T. Kouchoukos, MD,‡‡ Wistar Moore, MD,§§ Patrick M. McCarthy, MD,‖‖ Mehmet C. Oz, MD,¶¶ Francis Fontan, MD,## Meredith L. Scott, MD,§§ Kevin A. Accola, MD,§§ and the RESTORE Group

Birmingham, Alabama; Los Angeles, California; Monte Carlo, Monaco; Florence and Milan, Italy; Sao Paulo, Brazil; Freiburg, Germany; Charlottesville, Virginia; Kanagawa, Japan; St. Louis, Missouri; Orlando, Florida; Cleveland, Ohio; New York, New York; and Bordeaux, France

OBJECTIVES The purpose of this study was to test how surgical ventricular restoration (SVR) affects early and late survival in a registry of 1,198 post-anterior infarction congestive heart failure (CHF) patients treated by the international Reconstructive Endoventricular Surgery returning Torsion Original Radius Elliptical shape to the left ventricle (RESTORE) team.

BACKGROUND Congestive heart failure may be caused by late left ventricular (LV) dilation after anterior infarction. The infarcted segment is often akinetic rather than dyskinetic because early reperfusion prevents transmural necrosis. Previously, only dyskinetic areas were treated by operation. Surgical ventricular restoration reduces LV volume and creates a more elliptical chamber by excluding scar in either akinetic or dyskinetic segments.

METHODS The RESTORE group applied SVR to 1,198 post-infarction patients between 1998 and 2003. Early and late outcomes were examined, and risk factors were identified.

RESULTS Concomitant procedures included coronary artery bypass grafting in 95%, mitral valve repair in 22%, and mitral valve replacement in 1%. Overall 30-day mortality after SVR was 5.3% (8.7% with mitral repair vs. 4.0% without repair; $p < 0.001$). Perioperative mechanical support was uncommon (<9%). Global systolic function improved postoperatively. Ejection fraction (EF) increased from 29.6 ± 11.0% preoperatively to 39.5 ± 12.3% postoperatively ($p < 0.001$). The left ventricular end-systolic volume index (LVESVI) decreased from 80.4 ± 51.4 ml/m^2 preoperatively to 56.6 ± 34.3 ml/m^2 postoperatively ($p < 0.001$). Overall five-year survival was 68.6 ± 2.8%. Logistic regression analysis identified EF ≤30%, LVESVI ≥80 ml/m^2, advanced New York Heart Association (NYHA) functional class, and age ≥75 years as risk factors for death. Five-year freedom from hospital readmission for CHF was 78%. Preoperatively, 67% of patients were NYHA functional class III or IV and postoperatively, 85% were class I or II.

CONCLUSIONS Surgical ventricular restoration improves ventricular function and is highly effective therapy in the treatment of ischemic cardiomyopathy with excellent five-year outcome. (J Am Coll Cardiol 2004;44:1439–45) © 2004 by the American College of Cardiology Foundation

The etiology of congestive heart failure (CHF) is coronary artery disease in approximately two-thirds of cases. The majority of these patients have experienced myocardial infarction (1). Despite successful early reperfusion, late left ventricular (LV) dilation develops in 20% of patients and leads to CHF (2,3). Myocardial necrosis progresses sequentially in the untreated transmural infarction from endocardium to epicardium (4). Early reperfusion alters the infarction process by sparing the epicardial layer and preventing thin-walled dyskinetic aneurysm formation. The reperfused infarcted myocardium retains its thickness and normal epicardial appearance, resulting in an akinetic segment with varying degrees of mid-myocardial and epicardial fibrosis. The remote non-infarcted myocardium undergoes changes in volume and shape during the course of "ventricular remodeling." As the ventricle enlarges, its normal elliptical shape becomes spherical and global systolic function worsens, resulting in CHF (5). The prognosis of patients with

From the *Norwood Clinic and Kemp Carraway Heart Institute, Birmingham, Alabama; †UCLA Medical Center, Los Angeles, California; ‡Centre Cardiothoracique de Monaco, Monte Carlo, Monaco; §University of Florence, Florence, Italy; ‖Ospedale Clinicizzato San Donato, Milan, Italy; ¶University of Sao Paulo, Sao Paulo, Brazil; #Albert-Ludwigs-Universitat Freiburg, Freiburg, Germany; **University of Virginia, Charlottesville, Virginia; ††Shonan Kamakura General Hospital, Kamakura, Kanagawa, Japan; ‡‡Missouri Baptist Hospital, St. Louis, Missouri; §§Orlando Heart Surgery Group, Orlando, Florida; ‖‖The Cleveland Clinic Foundation, Cleveland, Ohio; ¶¶Columbia University, New York, New York; and ##St. Augustine Hospital, Bordeaux, France. Drs. Buckberg and Athanasuleas are consultants for Somanetics, and have a financial interest. Drs. Di Donato and Menicanti are consultants for Chase Medical. Dr. McCarthy is a consultant and has a financial interest with Myocor.

Manuscript received May 12, 2004; revised manuscript received June 24, 2004, accepted July 6, 2004.

Abbreviations and Acronyms

ACE	= angiotensin-converting enzyme
CABG	= coronary artery bypass grafting
CHF	= congestive heart failure
EF	= ejection fraction
LV	= left ventricular
LVAD	= left ventricular assist device
LVESVI	= left ventricular end-systolic volume index
NYHA	= New York Heart Association
SVR	= surgical ventricular restoration

ischemic cardiomyopathy is more closely related to LV volume rather than to ejection fraction (EF) (6).

The new term "surgical ventricular restoration" (SVR) includes operative methods that reduce LV volume and "restore" ventricular elliptical shape (7–9). Excision of a thin-walled aneurysm with direct closure is an early method of SVR first described by Cooley et al. (10,11) and modified over the years. This operation is rarely performed currently because early reperfusion spares epicardial muscle, resulting in regional thick-walled akinesia rather than thin-walled dyskinesia. Dor (12) recognized that the adverse effects of remodeling on the remote non-infarcted myocardium were similar for akinesia and dyskinesia and was the first to utilize the endocardial patch plasty procedure for both morphologies. Dor's (12) operation improves systolic function and New York Heart Association (NYHA) functional class (13). However, the operation is not widespread because surgeons have been unwilling to exclude the akinetic normal-appearing segments often encountered after early reperfusion. Instead, coronary artery bypass grafting (CABG) is performed and the non-functioning akinetic muscle segment containing deeper scar is left undisturbed.

The Reconstructive Endoventricular Surgery returning Torsion Original Radius Elliptical shape to the left ventricle (RESTORE) group is a team of cardiologists and surgeons from 12 centers on four continents: six in the U.S., four in Europe, one in South America, and one in Asia (Appendix). The following sections report on the RESTORE SVR registry with five-year follow-up and provide an update of our previous three-year findings in 439 patients (14).

METHODS

The SVR was performed in 1,198 patients between 1998 and 2003. Inclusion criteria were previous anterior myocardial infarction, significant ventricular dilation (left ventricular end-systolic volume index [LVESVI] $\geq$60 ml/m^2), and a regional asynergic (non-contractile) LV circumference of $\geq$35%. Patients were in NYHA functional class I in 9%, class II in 22%, class III in 40%, and class IV in 29% of cases. The small percentage of patients in class I underwent SVR while undergoing CABG or mitral repair as the primary operative indication, because LV volume exceeded 60 ml/m^2. Echocardiography, ventriculography, or magnetic resonance imaging was used to confirm the asynergic segment and calculate EF. The LVESVI was determined by ventriculography or magnetic resonance imaging. Institutional review board approval was not obtained because the investigators considered the operation an established therapy based on the acceptance of endoventricular circular patch plasty and the reported outcomes of Dor et al. (15).

Anteroseptal, apical, and anterolateral LV scarred segments were identified and excluded by an intracardiac patch or direct closure. The operation is illustrated in Figure 1. Patients were placed on cardiopulmonary bypass with moderate hypothermia (approximately 34°C). Hearts were protected with warm and cold-blood cardioplegia during coronary grafting and/or mitral procedures. The ventricular restoration portion of the operation was performed during cardioplegia-arrested heart by about half of the surgeons, and in the open-beating heart by the others. Postoperative EF and volumes were obtained before hospital discharge. Follow-up NYHA functional class was obtained during physician visit or by telephone interview.

Statistics. Analysis of survival and readmission probabilities versus volume, EF, and age were carried out using Kaplan-Meier survival analysis to properly account for patients lost to follow-up. A similar analysis was used to determine the effect of mitral valve repair, replacement, and readmission. Times were taken as times to first readmission for readmitted patients, time to death for non-readmitted patients who died, and time to last follow-up for all others. Patients lost to follow-up were removed from the study (censored) for Kaplan-Meier survival analysis as of the date of last follow-up. Data comparisons used the general linear model for numeric data and logistic regression for categorical data. The SAS Institute JMP 4.0 statistical package was used for all tests.

RESULTS

Baseline characteristics. Patient age ranged from 25 to 89 years with a mean of 63 $\pm$ 11 years. The interval between anterior infarction and SVR procedure averaged 4.4 years. Mean NYHA functional class was 2.9 preoperatively with 9% of patients in class I, 22% in class II, 40% in class III, and 29% in class IV. Akinesia was present in 66% of cases and dyskinesia in 34%. Larger ventricular volumes were noted in patients with akinetic segments. Among the ventricles with LVESVI $\geq$80 ml/m^2, akinesia was present in 73.3% and dyskinesia in 26.7%.

Concomitant procedures included CABG in 95%, mitral valve repair in 22%, and mitral valve replacement in 1%. Patients undergoing mitral valve procedures had reduced EF and larger ventricles compared with patients in whom no mitral procedure was performed. If EF was $\leq$30%, mitral valve procedures were performed in 33.3% versus 15.0% in patients whose EF was >30% ($p < 0.0001$). Among patients with LVESVI $\geq$80 ml/m^2, mitral procedures were more common as compared with patients with smaller volumes (34.1% vs. 21.1%, $p < 0.0001$).

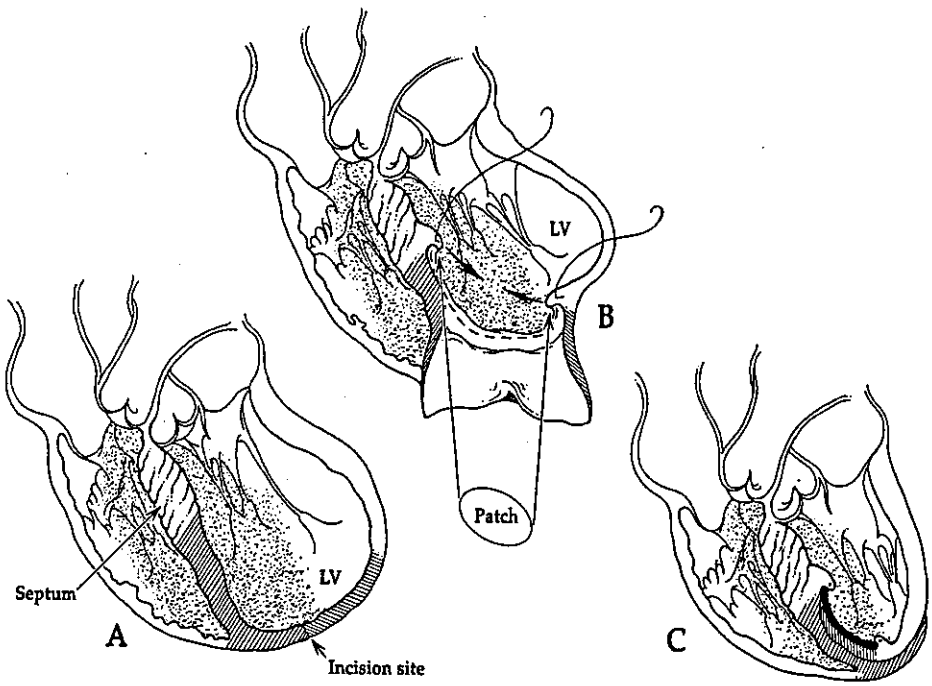

Figure 1. **(A)** Incision into the scar of the dilated ventricle. **(B)** Placement of a suture to exclude the scarred segment. **(C)** Completed repair with endocardial patch. LV = left ventricle.

Early outcome. Global systolic function improved postoperatively. The EF, measured in 1,118 patients before discharge from the hospital, increased from 29.6 ± 11.0% preoperatively to 39.5 ± 12.3% postoperatively ($p < 0.001$). Both preoperative and postoperative EF were significantly less for patients undergoing mitral valve repair. There was no difference between the groups in improvement in EF (Table 1).

The LVESVI, obtained in 671 patients, was reduced from 80.4 ± 51.4 ml/m^2 preoperatively to 56.6 ± 34.3 ml/m^2 postoperatively ($p < 0.001$). Normal LVESVI is 24 ± 10 ml/m^2 (16). Patients undergoing mitral valve repair had significantly larger hearts preoperatively than those with no mitral valve repair. There was no difference in postoperative LVESVI between the groups. Improvement in LVESVI was significantly greater in patients undergoing mitral valve repair (Table 2).

Thirty-day mortality after SVR was 5.3%, and it was higher among patients undergoing concomitant mitral valve repair (8.7%) versus patients in whom no mitral valve procedure was required (4.0%, $p < 0.001$). Perioperative mechanical support was uncommon; intra-aortic balloon pumping was used in 8.2%, left ventricular assist device (LVAD) in 0.7%, and extracorporeal membrane oxygenation in 0.3%.

To assess inter-institutional differences in outcome, the centers were arranged in order of increasing preoperative risk, as determined by logistic regression of a combination of preoperative NYHA functional class, EF, LVESVI, and age on survival. Incomplete data excluded some patients from this analysis. There was a nearly linear relationship between risk and five-year survival for all centers for which meaningful risks could be calculated.

Late outcome. Overall five-year survival was 68.6 ± 2.8%, calculated by the Kaplan-Meier product-limit method (Fig. 2). Mean time to death or loss to follow-up was 1.85 ± 1.45 years; at the end of five years, 22 patients remained in the study. Survival at five years was better in the group of patients that had dyskinetic as compared with akinetic morphology (80% vs. 65%; $p < 0.001$) (Fig. 3). Logistic regression analysis identified risk factors for death at any time after surgery. These included preoperative EF ≤30%, LVESVI ≥80 ml/m^2, advanced NYHA functional class, and age ≥75 years. Patients with EF ≥30% had survival 76.7 ± 3.2% as compared with 63.8 ± 3.9% for those with EF ≤30% (Fig. 4). Patients with EF >40% had survival

Table 1. LVESVI (ml/m^2) and Mitral Valve Repair

	No Mitral Repair	Mitral Repair	p Value
Preoperative	76.3	89.4	< 0.006
Postoperative	56.0	55.8	NS
Change	20.3	33.6	< 0.002

LVESVI = left ventricular end-systolic volume index.

Table 2. EF (%) and Mitral Valve Repair

	No Mitral Repair	Mitral Repair	p Value
Preoperative	31.0	25.4	< 0.0001
Postoperative	41.3	34.0	< 0.0001
Change	10.3	9.3	NS

EF = ejection fraction.

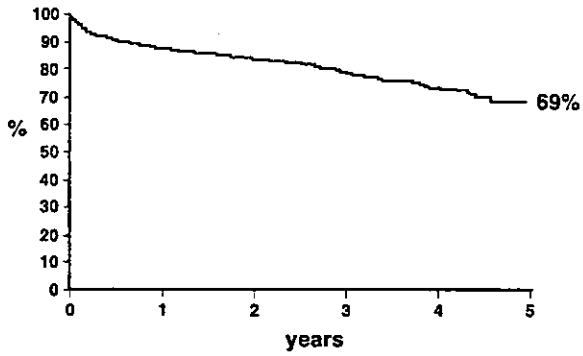

Figure 2. Overall five-year survival.

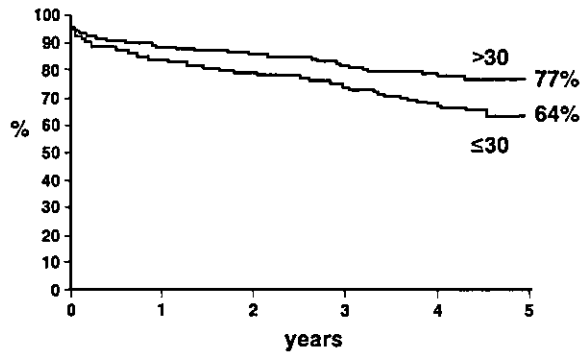

Figure 4. Survival based upon preoperative ejection fraction.

83.0 ± 4.0% as compared with 67.4 ± 3.0% for those with EF ≤40% ($p < 0.001$). Patients with LVESVI <80 ml/m^2 had survival 79.4 ± 3.3% as compared with 67.2 ± 3.2% for those with hearts >120 ml/m^2 ($p < 0.001$) (Fig. 5). Preoperative NYHA functional class was associated with long-term survival. At five years, survival was 94.5 ± 2.7% in NYHA functional class I, 87.2 ± 3.3% in class II, 69.9 ± 4.7% in class III, and 49.7 ± 5.8% in class IV ($p < 0.001$) (Fig. 6).

Mitral valve procedures were performed more commonly in patients with larger ventricles and reduced EF. Mortality at 30 days was higher in patients who underwent concomitant mitral repair (9.1%) as compared with those in whom no mitral valve procedure was performed (4%; $p < 0.001$). However, at five years, the survival curves were not different between patients who underwent repair and those who did not (68.7 ± 3.9% vs. 70.8 ± 3.3%). Mitral valve replacement was rare (30 patients, <1%) and was performed early in the registry. These patients had extensive areas of remote muscle scar precluding simple annuloplasty to correct mitral regurgitation.

Freedom from readmission to the hospital for CHF was 78%. The NYHA functional class improved from a mean of 2.9 preoperatively to 1.7 postoperatively. Preoperatively, 67% of patients had NYHA functional class III or IV symptoms (39% class III, 28% class IV). Postoperatively, 85% were functional class I or II (48% class I, 37% class II).

SVR in the elderly. Age was also a risk factor. Among all patients operated on, 12.4% (149) were ≥75 years old.

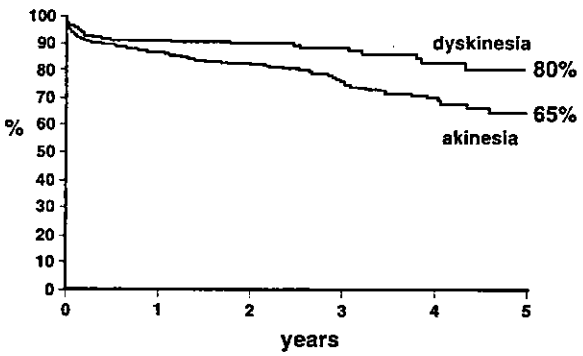

Figure 3. Survival based upon chamber morphology: dyskinesia versus akinesia.

Concomitant procedures included coronary bypass in 98%, mitral valve repair in 17%, and replacement in 4%. Mortality 30 days after operation was 13% and higher than in younger patients. Postoperative hemodynamic support with intra-aortic balloon pumping was required in 13%. The EF improved from 31% preoperatively to 39% postoperatively ($p < 0.001$). The LVESVI was reduced from 88 ml/m^2 to 60 ml/m^2 ($p < 0.001$). Overall five-year survival in the elderly was 63% and related to preoperative EF (50% if preoperative EF <30% and 73% if EF ≥30%; $p < 0.001$). Among elderly patients undergoing concomitant CABG, the five-year survival was 71% compared with 55% among patients undergoing simultaneous mitral valve procedures. The NYHA functional class III and IV was present in 70% of patients preoperatively and in 20% postoperatively. Mean NYHA functional class improved from 3.0 to 1.9. Hospital readmission for CHF at five years was 15%.

DISCUSSION

Remodeling after infarction enlarges chamber diameter and increases wall tension by Laplace's law. The augmented wall stress results in increased oxygen consumption, decreased subendocardial blood flow, and reduced systolic shortening. White et al. reported that LV volume was more predictive of survival than EF after infarction (6). Investigators in the Global Utilization of Streptokinase and t-PA for Occluded Coronary Arteries (GUSTO I) trial confirmed this and showed that LVESVI ≥40 ml/m^2 after infarction was associated with high CHF rates and poor long-term survival (3). The SVR reshapes the remodeled LV and significantly reduces chamber volume.

Ventricular shape in dilated cardiomyopathy is also an important determinant of function. As the enlarging LV changes from elliptical to spherical, normal systolic torsion is reduced. The myofibrils of the spherical LV are shifted away from their normal oblique axis toward a more transverse direction. The normal myofibril shortening of 15% generates a global EF of only 30% in spherical ventricles, as compared with an EF of 60% in elliptical ventricles with natural torsion (17). The circumferential radius of curvature increases after infarction with loss of regional EF in the remote non-infarcted myocardium (18). The Dor procedure

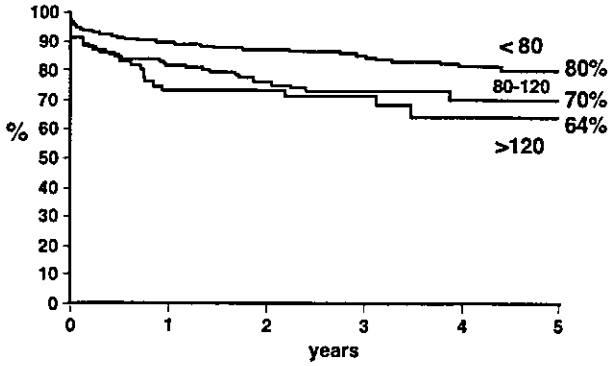

Figure 5. Survival based upon preoperative left ventricular end-systolic volume index.

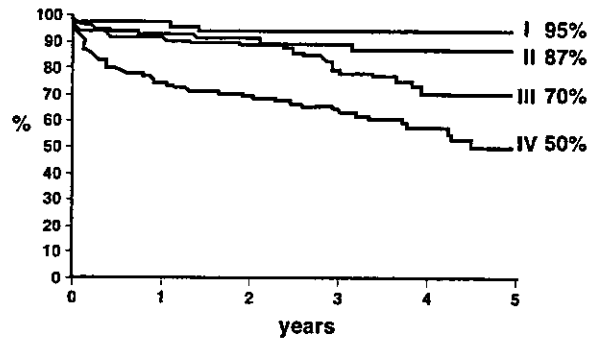

Figure 6. Survival based upon preoperative New York Heart Association functional class.

improves global systolic function by increasing regional function in remote non-infarcted segments (19). Postoperatively, LV shape becomes more elliptical in systole than it was in diastole (20).

In this RESTORE registry, SVR was used to correct LV geometry in all cases. Concomitant procedures included CABG in 95% and mitral valve intervention in 23%. Thus, the three pathologic components contributing to CHF—the ventricle, vessel, and valve—were all surgically corrected. Our integrated approach resulted in an overall five-year survival of approximately 70% and a rehospitalization for CHF of 22%. These results can be contrasted to current approaches including medical therapy, CABG alone, CABG with mitral intervention, ventricular assist devices, and transplantation.

Medical therapy. Angiotensin-converting enzyme (ACE) inhibitors increase survival among NYHA functional class IV CHF patients as shown in the Cooperative North Scandinavian Enalapril Survival Study (CONSENSUS) trial; however, only 64% survived to one year (21). Although the Carvedilol Prospective Randomized Cumulative Survival (COPERNICUS) trial demonstrated an advantage of adding carvedilol to ACE drugs in patients with EF <25%, survival at 28 months was 72% (22). Recently, the Carvedilol or Metoprolol European Trial (COMET) trial examined the efficacy of carvedilol in NYHA functional class III (48%) and IV (3%) patients with a mean EF of 26%. Survival at five years was 66% in the carvedilol treated group (23). In the Carvedilol and ACE Inhibitor Remodeling Mild Heart Failure EvaluatioN (CARMEN) trial, the majority of patients were NYHA functional class II (60% to 70%) and there were none in class IV. Event-free mortality or hospitalization was approximately 75% at two years with marginal reduction of LVESVI (7 ml/m^2) and EF improvement of 3.5% (24). Recently, spironolactone was added to ACE and beta-blocker therapy in the Randomized Aldactone Evaluation Study (RALES) trial among patients with EF ≤35%. Pre-treatment class was not reported, but the two-year survival was 65% in the treated group versus 54% in the placebo group (25).

In contrast to the above-cited trials, our RESTORE registry provides five-year follow-up in patients whose NYHA functional class was III or IV in 67% of cases. Systolic function was measured by EF and ventricular volume. Both showed dramatic improvement. Rehospitalization was very low in a high-risk patient population.

Coronary revascularization. Coronary artery bypass grafting can be safely carried out in patients with reduced systolic function because of improved methods of myocardial protection; however, the five-year survival of patients with EF ≤35% is 50% to 65% (26–29). The CABG alone is not very effective when ventricular dilation occurs. In one study, CABG mortality was 27% if LV end-diastolic diameter was ≥81 mm (30). Moreover, CHF symptoms are common after CABG for ischemic cardiomyopathy. Yamaguchi's analysis of CABG for patients with EF ≤30% showed that outcome correlated with preoperative LVESVI. The five-year survival was 54% if the preoperative LVESVI was ≥100 ml/m^2 compared with 85% if LVESVI was ≤100 ml/m^2. Congestive heart failure at five years was seen in 69% of patients with the larger hearts versus 15% with the smaller ones (31). Luciani et al. reviewed 167 patients who underwent CABG with a mean EF of 28%. Among these patients, 40% were functional class III or IV. At five years, 60% of patients continued to have signs and symptoms of CHF, demonstrating the limitations of CABG surgery alone (32). Another study of CABG for ischemic cardiomyopathy confirmed that recurrent CHF was the most common cause of death postoperatively (27).

Mitral valve repair or replacement. Functional mitral regurgitation often accompanies ventricular dilation (33). Patients with ischemic cardiomyopathy undergoing mitral procedures have a five-year mortality of approximately 50% (27,34). Recurrence of CHF occurs in one-third of patients by five years and is the most common cause of death, presumably related to continuing dysfunction of the unmodified ventricle (27,35). Mitral valve repair is an integral part of the SVR procedure in addition to volume reduction and revascularization.

Ventricular assist or replacement. Other surgical approaches in the treatment of ischemic cardiomyopathy include LVAD and transplantation. The Randomized Evaluation of Mechanical Assistance for the Treatment of